PERGAMON

Journal of Structural Geology 24 (2002) 1677–1698

JOURNAL OF STRUCTURAL GEOLOGY

www.elsevier.com/locate/jstrugeo

Offset and evolution of the Gowk fault, S.E. Iran: a major intra-continental strike-slip system

Richard Walker*, James Jackson

Bullard Laboratories, Madingley Road, Cambridge CB3 0EZ, UK

Received 15 March 2001; revised 12 September 2001; accepted 5 December 2001

Abstract

We use drainage reconstructions to estimate long-term offsets on the Gowk fault, an oblique right-lateral strike-slip fault in eastern Iran, on which there have been a number of recent large earthquakes. A 3 km horizontal offset is inferred from well-preserved geomorphology. We further identify a total cumulative offset of ~12 km, which produces a simple reconstruction of geomorphology across the fault, filling in pull-apart basins, restoring rivers to linear courses across the fault trace and aligning structural and bed-rock features. The probable age of the Gowk fault, and K–Ar dating of offset basalts north of the study region, suggest an overall slip rate of ~1.5–2.4 mm/year. This is small compared with the overall 10–20 mm/year of shear expected between central Iran and Afghanistan and the deficit is likely to have been accommodated on other faults east of the Gowk fault. Drainage displaced by dextral movement leads to the development of a series of basins along the fault and a longitudinal topographic profile that resembles an asymmetric saw-tooth. The geomorphic evolution of the fault zone at the surface includes both normal and reverse faulting components, reflecting a probable ramp-and-flat structure in cross-section. This interpretation is consistent with evidence from the analysis of seismological, radar and surface rupture data in recent earthquakes.

Keywords: Active tectonics; Eastern Iran; Drainage reconstructions; Strike-slip faulting

1. Introduction

This paper has two aims. One is to estimate the late-Tertiary offset on a large active strike-slip fault system, which accommodates the shear between central Iran and Afghanistan that arises because of the Arabia–Eurasia collision. Knowing the offset on the fault system will help us understand how that shear is achieved, which is an important aspect of Middle East active tectonics. The other aim is to understand the three-dimensional structure of the strike-slip zone and how it evolves with time. The fault zone is active now, having produced three earthquakes of $M_s > 6$ in the last 20 years, and we can use the seismological information from these earthquakes to constrain the fault geometry at depth. In addition, because movement on the faults is the dominant control on the drainage and geomorphology, we can use the development of the landscape to infer both the structure and sense of motion of the faults today and also how they have evolved with time. It is this very close link between geomorphology and structure on active faults that Bayasgalan et al. (1999a,b) exploited on large strike-slip faults in Mongolia.

This paper concentrates on the Gowk section of the Nayband–Gowk fault system in SE Iran (Figs. 1 and 2). We first summarize the tectonic and geological setting of this system, and its role in the active tectonics of Iran. We then examine the evidence for offsets on the Gowk fault, using the drainage and morphology. Next we show how the evolution of the geomorphology contains information about the structure and growth of the fault zone. Finally we examine evidence for offsets elsewhere on the Nayband–Gowk fault system and for information that may help estimate slip rates, before discussing the significance of these results for the regional tectonics.

2. Tectonic and geological setting of the Gowk fault

2.1. Active tectonics

The Iran–Afghanistan border region is the eastern extremity of the Arabia–Eurasia collision zone. At this longitude nearly all the Arabia–Eurasia shortening is accommodated within the political borders of Iran itself

* Corresponding author.
E-mail addresses: rwalker@esc.cam.ac.uk (R. Walker), jackson@esc.cam.ac.uk (J. Jackson).

0191-8141/02/$ - see front matter
PII: S0191-8141(01)00170-5

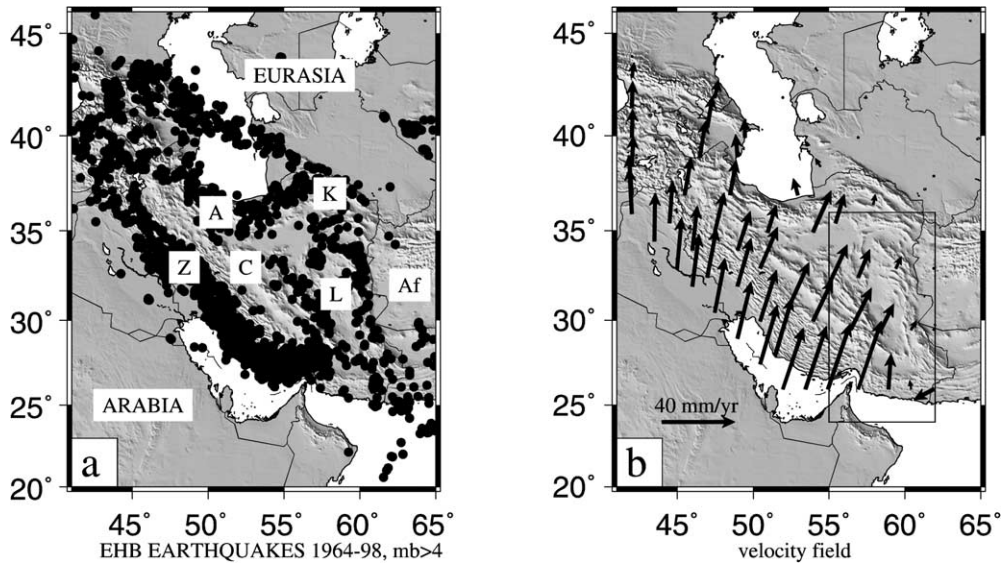

Fig. 1. (a) Seismicity of Iran for the period 1964–1990. Epicentres are from Engdahl et al. (1998). The seismicity is mainly confined within the political borders of Iran with Eurasia and Afghanistan (Af) being essentially aseismic. Earthquake deformation within Iran is concentrated in the Zagros (Z), the Alborz (A), the Kopet Dag (K) and in eastern Iran. The aseismic central Iran and Lut blocks are denoted by C and L. (b) A velocity field for Iran estimated from the spatial variation in the style of strain rates indicated by earthquakes (from Jackson et al. (1995)). Velocities are shown relative to stable Eurasia. Note the right-lateral shear expected along the eastern border of Iran. The boxed region shows the area of Fig. 2.

(Fig. 1). Western Afghanistan is virtually aseismic and essentially a promontory of Eurasia, which extends to the Indian Ocean in the Makran subduction zone. Some of the Arabia–Eurasia convergence is accommodated in the Zagros mountains of SW Iran, while most of the rest is taken up in the seismic belts of the central Caspian, the Alborz and the Kopeh Dag of northern Iran, as central Iran itself is relatively flat, aseismic, and probably rigid. Whatever shortening is not taken up in the Zagros must be expressed as N–S right-lateral shear between central Iran and Afghanistan. This shear is manifest by major N–S right-lateral fault systems on both the west (in Kerman province) and east (in Sistan) sides of the Dasht-e-Lut, another flat, aseismic rigid block (Fig. 2). The amount of this shear, how it is distributed, and the relative importance of the two strike-slip systems either side of the Lut, are questions addressed in this paper.

The overall Arabia–Eurasia convergence is known from a combination of Africa–Eurasia and Arabia–Eurasia motions to be approximately N–S in eastern Iran, with rates of about 30 mm/year at 50°E and 40 mm/year at 60°E (Jackson, 1992; DeMets et al., 1994; Jestin et al., 1994; Chu and Gordon, 1998). Central Iran is a mosaic of various tectonic blocks once separated by minor ocean basins (Berberian and King, 1981) that started to close in the mid-Tertiary (McCall, 1996). Much of the broader collision zone, however, did not start to deform until the Mid-Miocene or even later (Dewey et al., 1986). In particular, major deformation of the Zagros folded belt appears not to have begun until the Pliocene, ~5 Ma years ago or less (Falcon, 1974), which is also the time at which there was a major re-organization of the sedimentation and deformation in the South Caspian Basin (Devlin et al., 1999; Jackson et al., 2002). We suspect this time represents the final closure of any remaining ocean basins and the onset of true intra-continental shortening within Iran. We also expect that the present-day configuration of active faulting dates from roughly this time. Jackson and McKenzie (1984, 1988) and Jackson et al. (1995) suggest that the Zagros accommodates about 10–15 mm/year of present-day shortening. This estimate is very dependent on the assumptions they made, but is roughly compatible with ~50 km of shortening thought to have occurred in the folded belt of the Zagros over the last 5 Ma (Falcon, 1969, 1974). Thus we expect that 20–25 mm/year remains to be taken up north of the Zagros and to be represented as N–S shear in eastern Iran. This reasoning implies that a total of 100–125 km of right-lateral slip has occurred on the faults east and west of the Dasht-e-Lut over the last 5 Ma; the total offset may be more if the faults were active before 5 Ma. Currently there are no field-based estimates of late Tertiary offsets on the faults west of the Dasht-e-Lut. East of the Dasht-e-Lut, Freund (1970) suggests offsets of 13 km on the Zahedan fault and Tirrul et al. (1983) estimate ~60 km of cumulative offset on the Neh fault system (Fig. 2).

This paper is concerned with the Nayband–Gowk fault system on the west side of the Dasht-e-Lut (Fig. 2). We concentrate particularly on the Gowk section (Figs. 2 and 3) for two reasons. First, a number of substantial earthquakes that involved surface rupture occurred on this part of the fault system in the last 20 years (Berberian et al., 1984, 2001), so that we have some knowledge of its subsurface structure. Second, the Gowk fault contains some remarkable geomorphology that allows us to reconstruct

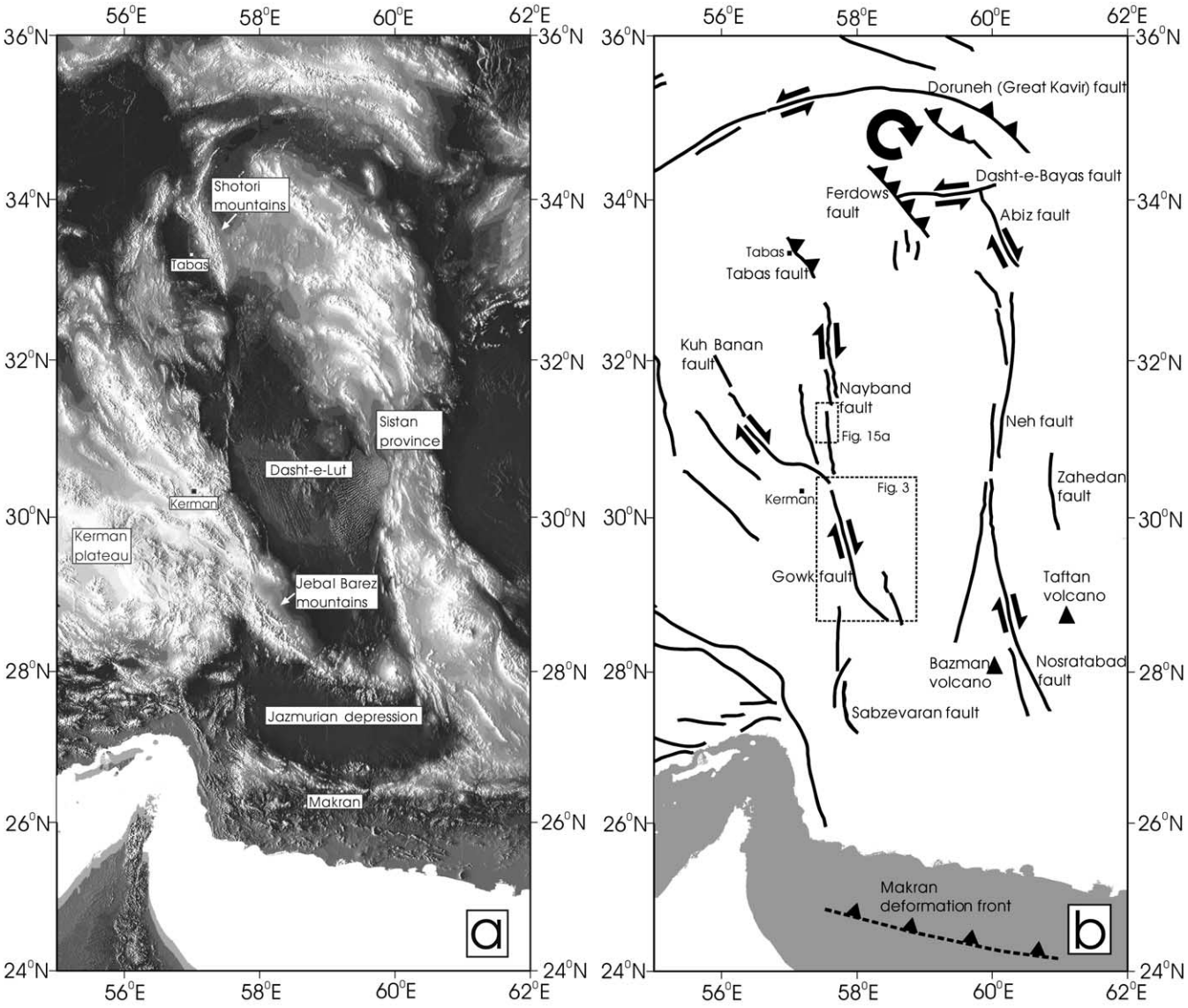

Fig. 2. (a) Regional topographic map of eastern Iran. Note the narrow N–S mountain ranges bordering the Dasht-e-Lut depression. (b) Major faulting in eastern Iran. South of 34°N deformation occurs in two zones of N–S dextral strike-slip, which follow the narrow mountain ranges of Fig. 2a. North of 34°, E–W left-lateral faulting predominates. Boxes show the areas of Figs. 3 and 15.

its offset and evolution with time, and also gives us insights into how drainage systems respond to strike-slip faulting that may be applicable elsewhere. As is commonly the case, it is difficult to find datable markers that can turn offset measurements into slip rates. But (to anticipate one of our conclusions), the available evidence is nonetheless sufficient to suggest the probable slip rates (~1–2 mm/year) and total offset (~12 km) on the Nayband–Gowk fault system are relatively small, and that most of the N–S shear between central Iran and Afghanistan is taken up on the eastern side of the Dasht-e-Lut.

2.2. Topography

Strike-slip faulting on the west side of the Lut extends over a N–S distance of nearly 600 km and occurs in three main sections: the Nayband fault in the north, the Sabzevaran fault in the south and the Gowk fault in the middle (Fig. 3). At its northern end, this system appears to connect with the Tabas thrust system bounding the Shotori mountains (Fig. 2), while in the south it ends in the Makran (Fig. 2). The Gowk fault itself dies out in the Jebal Barez mountains, which themselves merge with the active volcanic arc north of the Makran subduction zone (Fig. 3). Whereas the Nayband and Sabzevaran faults strike ~175° and produce simple linear scarps associated with almost no topographic step, the Gowk fault strikes ~155° and forms a more complex system of fractures and scarps in a narrow linear valley with major mountains on either side (Fig. 3). If we assume that the lack of topographic contrast across the Nayband and Sabzevaran faults indicates that the regional slip vector is ~175°, then the 155° strike of the Gowk fault

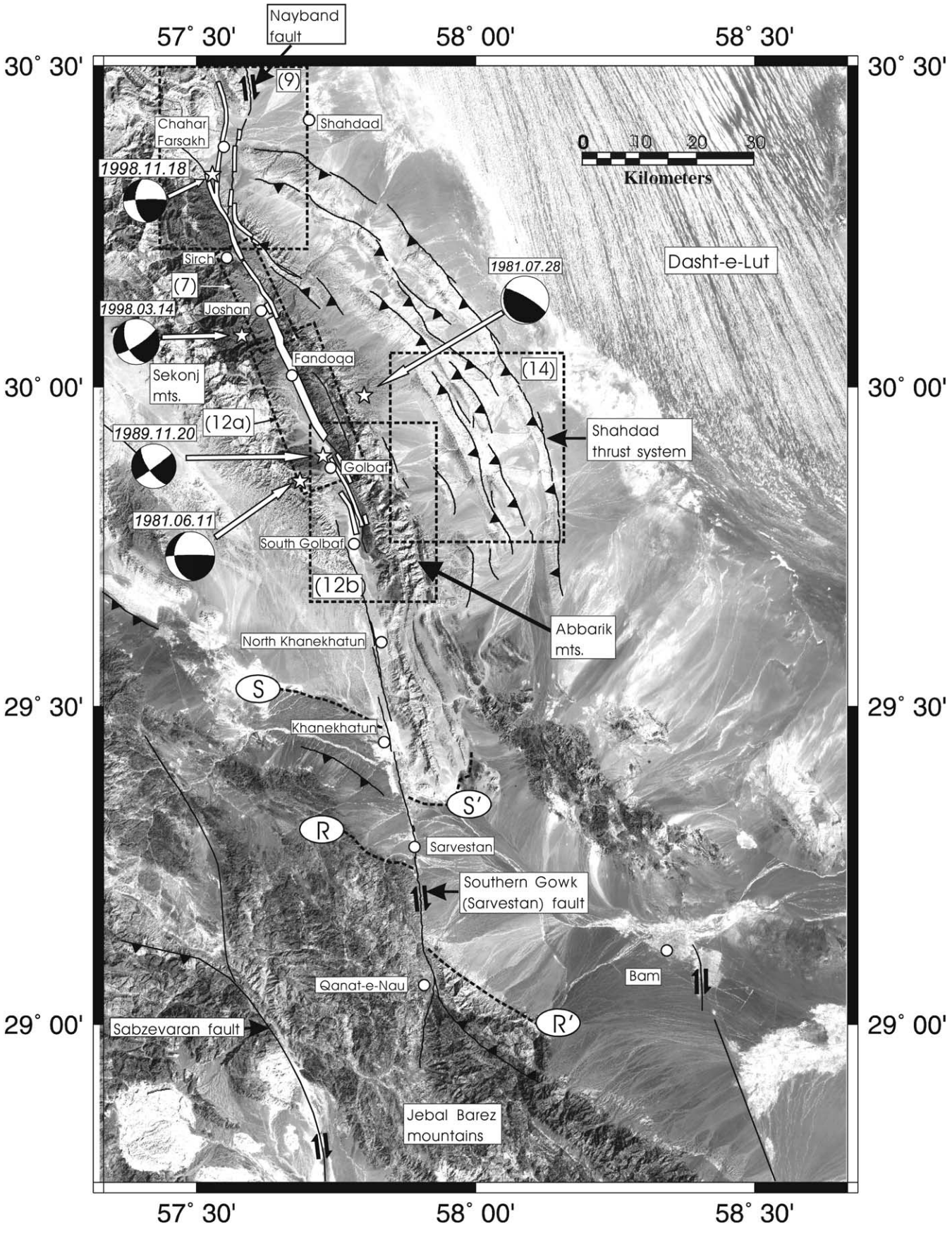
57° 30'
58° 00'
58° 30'
30° 30'
30° 00'
29° 30'
29° 00'
Nayband fault
(9)
Shahdad
Chahar Farsakh
1998.11.18
0 10 20 30
Kilometers
Dasht-e-Lut
Sirch
(7)
1998.03.14
Joshan
1981.07.28
Fandoqa
(14)
Sekonj mts.
(12a)
Shahdad thrust system
1989.11.20
Golbaf
1981.06.11
South Golbaf
(12b)
Abbarik mts.
North Khanekhatun
S
Khanekhatun
S'
R
Sarvestan
Southern Gowk (Sarvestan) fault
Bam
Qanat-e-Nau
R'
Sabzevaran fault
Jebal Barez mountains

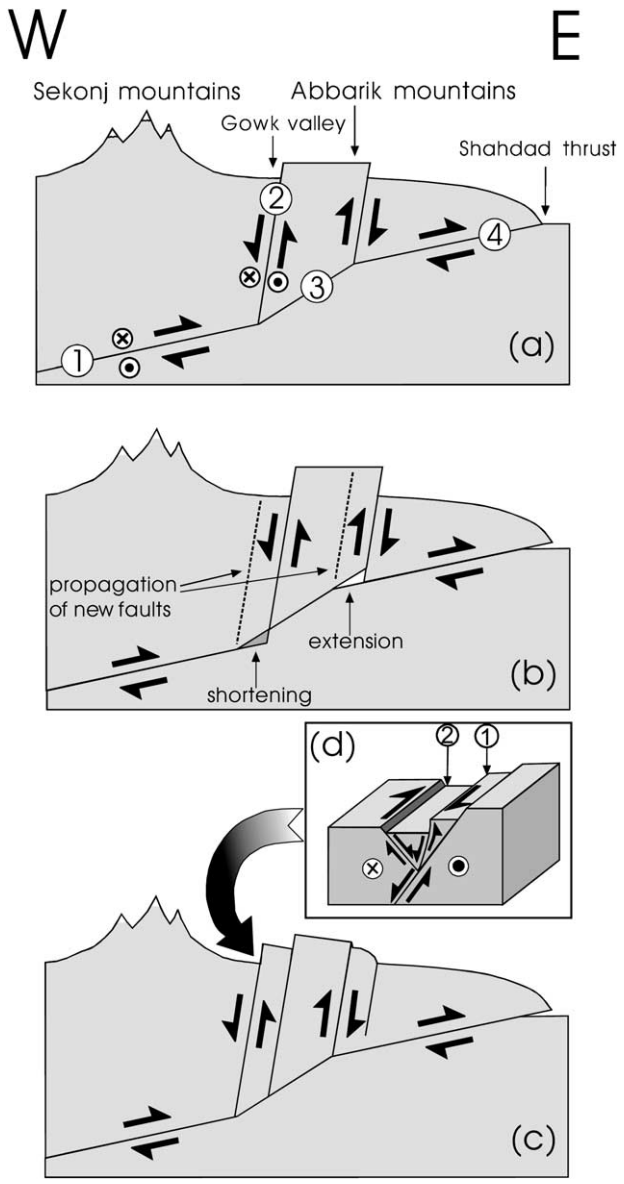

Fig. 4. (a) Structure of the Gowk fault as proposed by Berberian et al. (2001). Gently-dipping parts of the system (1 and 4) are separated by a steeper 'ramp' (3) that causes uplift of the Abbarik mountains and localised oblique normal faulting (2) in the Gowk valley. Sections (3) and (4) show purely thrust motion. (b) Fault movement causes zones of shortening and extension. We might therefore expect a westward propagation of active faulting in the Abbarik mountains, as shown in (c). (d) Movement on a westward-dipping fault can give rise to east-facing scarps, as are seen in the Golbaf valley, where near-surface tensional failure of unconsolidated alluvium causes a fissure to open above the fault (1), accompanied by eastward slumping of the unconsolidated material (2).

would require a component of shortening. Evidence for shortening is contained in a series of parallel anticlines associated with blind thrusts to the east of the Gowk fault, called the Shahdad thrust system (Fig. 3). The Gowk valley and its associated faulting roughly follows the border between the Kerman plateau and the Dasht-e-Lut (Fig. 2), but is not a single structure at the base of the topographic slope. West of the Gowk valley the Sekonj mountains rise to heights of 4200 m, at least 1500 m above the plateau level. East of the valley the steep Abbarik mountains reach heights of 2700 m. The Gowk valley floor itself is typically at elevations of 1700–2000 m and is suspended above the much lower desert floor to the east (200–500 m).

2.3. Geology

The Sekonj mountains west of the Gowk fault consist of gently folded Mesozoic and Tertiary flysch sediments ranging from Senonian to Paleocene in age. Jurassic siltstones and sandstones also outcrop. East of the fault the Abbarik mountains typically contain tightly folded and faulted Cretaceous sediments thrust eastwards over a magmatic arc assemblage of Eocene volcanics and Paleogene pyroclastics. Precambrian salt deposits equivalent in age to the Hormuz salt of the Zagros are exposed in the Kuh Banan and Lakar Kuh mountains 75 km NW of Shahdad, but none are known to occur in the Gowk region. The Dasht-e-Lut depression contains several hundred meters of upper Pliocene to Pleistocene lacustrine silts over a basement of flat-lying Paleogene andesitic lavas and tuffs. Several Quaternary basalt flows occur near the Nayband fault on the western edge of the Lut. The arcuate anticline ridges of the Shahdad thrust belt are formed in up to 3000 m of stratified marls containing gypsum, sandstone and conglomerates, which onlap the eastern margin of the Abbarik mountains (Dimitrijevic, 1973; Sahandi, 1992; Aghanabati, 1993).

2.4. Earthquakes

The Gowk fault has been associated with five earthquakes of $M_w = 5.4–7.1$ in the last 20 years (Fig. 3), in contrast to the Nayband and Sabzevaran faults to the north and south, for which there is no historical evidence of seismicity over the last 1000 years (Ambraseys and Melville, 1982; Berberian and Yeats, 1999). The main features of the earthquakes between 1981 and 1998 have been described by

Fig. 3. LANDSAT TM image and location map of the Gowk fault region. The Sekonj and Abbarik mountains bound the fault to west and east, respectively. Drainage is directed eastwards from the Sekonj mountains through the Abbarik mountains to the Dasht-e-Lut. Lines S–S′ and R–R′ highlight a distinct soil change and a mountain range-front displaced by fault movement, respectively (see "Electronic Supplements" on the journal's homepage: http://www.elsevier.com/locate/jstrugeo). White lines represent 1981 surface ruptures. Those south of Golbaf are associated with the 11 June Golbaf earthquake ($M_w = 6.6$) and those north of Golbaf with the 28 July Sirch event ($M_w = 7.1$). Some surface ruptures south of Golbaf were re-activated by the 1989 South Golbaf event ($M_w = 5.8$). The March 1998 Fandoqa earthquake ($M_w = 6.6$) re-ruptured a 23 km section of the 1981 surface breaks along the thickened white line. Minor surface faulting was associated with the November 1998 earthquake ($M_w = 5.4$) near Chahar Farsakh. Epicentres are from Engdahl et al. (1998), and may be in error by 10–20 km. In particular, the 1981/07/28 Sirch earthquake began with a small sub-event preceding the main moment release by ~4 s (Berberian et al., 1984), so its location determined by arrival times is not likely to be representative of the main rupture. Fault-plane solutions for the South Golbaf (1989/11/20) and Fandoqa (1998/03/14) earthquakes are from Berberian et al. (2001). The rest are from the Harvard CMT catalogue. Dashed boxes show positions of later figures.

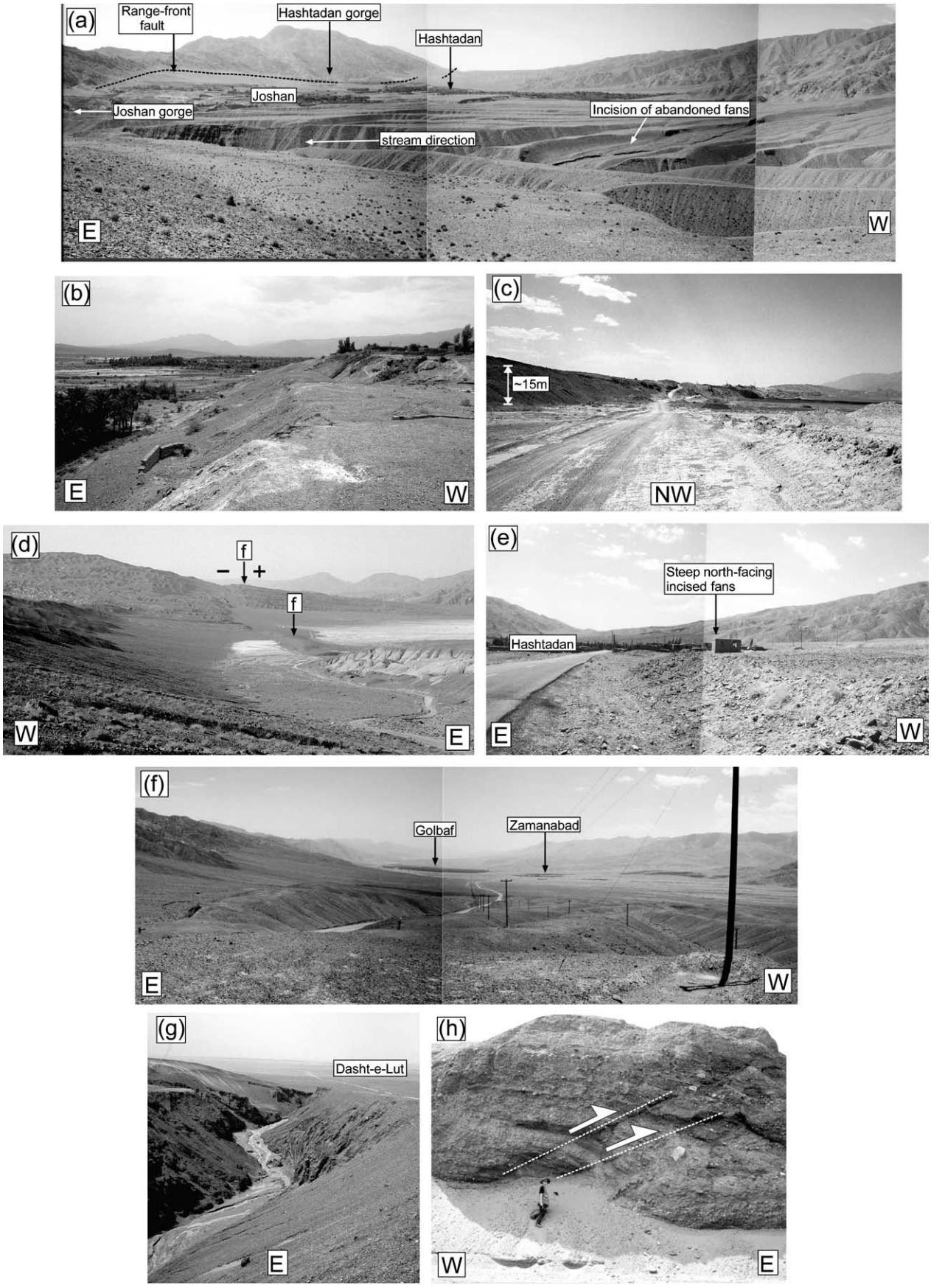
(a)
Range-front fault
Hashtadan gorge
Hashtadan
Joshan
Joshan gorge
Incision of abandoned fans
stream direction
E
W
(b)
E
W
(c)
~15m
NW
(d)
f
– +
f
W
E
(e)
Steep north-facing incised fans
Hashtadan
E
W
(f)
Golbaf
Zamanabad
E
W
(g)
Dasht-e-Lut
E
(h)
W
E

Berberian et al. (1984, 2001) and Berberian and Qorashi (1994), and provide an overview of the structure of the Gowk fault zone.

The 14 March 1998 Fandoqa ($M_w = 6.6$) earthquake ruptured 23 km of the Gowk fault centered on Fandoqa, with an average right-lateral slip of ~1.3 m but with surface displacements up to 3 m in places. Analysis of long-period seismic bodywaves and radar interferograms shows that the earthquake ruptured a fault dipping west at ~50° to a depth of 7–10 km, with a small normal component and a slip vector azimuth of ~147° (Berberian et al., 2001). In addition, radar interferograms show that the part of the Shahdad thrust system immediately east of the 1998 ruptures in the Gowk valley also moved about 8 cm on a fault dipping 6°W between depths of ~1 and 5 km, in a time interval that makes it likely that the slip on the thrust was triggered by the strike-slip earthquake. The slip vector azimuth on the thrust was about 062°, nearly perpendicular to that on the strike-slip fault. The oblique shortening across the Gowk fault system, required by its general trend of 155°, therefore appears to be achieved by a spatial separation ('partitioning') of the strike-slip and reverse components onto adjacent, sub-parallel faults.

Two earlier large earthquakes occurred in 1981. The 11 June 1981 Golbaf earthquake ($M_w = 6.6$) produced 15 km of right-lateral ruptures south of Golbaf, but with very small surface displacements of up to 3 cm. The much larger ($M_w = 7.1$) 28 July 1981 Sirch earthquake produced 65 km of discontinuous right-lateral surface ruptures between Golbaf and Chahar Farsakh (Fig. 3), in places following precisely the trace of the future 1998 Fandoqa earthquake but with maximum displacements of less than 50 cm. Berberian et al. (2001) suggest that the overall structure of the Gowk fault system in cross-section is that of a ramp-and-flat thrust (Fig. 4a) but with strike-slip motion superimposed. They suggest that the 1981 earthquakes ruptured a deeper flatter part of the system (1), which later failed on a steeper shallower fault (2) in 1998. In their scheme, the steeper ramp (3) underlies the Abbarik mountains, while the upper flat part of the thrust system (4) underlies the Shahdad anticlines. With this configuration of faulting the Abbarik mountains east of the Gowk valley are being uplifted as they move over the steep 'ramp' of the fault system. We examine the geomorphological evidence for this geometry and its evolution later.

2.5. Drainage

The key to understanding the offsets and evolution of the Gowk fault is the drainage. The regional drainage flows off the high Sekonj mountains in the west to eventually reach the Lut depression in the east. But to do so it must first cross the Gowk valley. The valley itself is generally 2–4 km wide and varies substantially in elevation along the length of the fault, with a series of depressions typically separated by incised alluvial fans forming topographic barriers and local drainage divides. The depressions are, from north to south, at Chahar Farsakh, Sirch, Joshan, Fandoqa, Golbaf, South Golbaf, North Khanekhatun and Khanekhatun (Fig. 3). Rivers that feed into the Gowk valley from the Sekonj mountains in the west either end in internally draining depressions within the valley (e.g. at Fandoqa) or flow parallel to the valley axis until reaching one of three currently open gorges through the Abbarik mountain range near Sirch, Joshan and Golbaf. The rivers exiting these three gorges then flow east across the growing anticlines of the Shahdad thrust system to reach the Dasht-e-Lut, which is the regional base-level and is both internally draining and extremely arid.

Various factors therefore affect the courses of the river systems. The Gowk valley exists as a topographic low because of the small up-to-the-east normal component on the Gowk fault (as seen in the 1998 Fandoqa earthquake), which causes it to be a sink into which the rivers deposit large alluvial fan systems (e.g. Fig. 5a). Meanwhile the gorges that cross the Abbarik mountains in the east are being (relatively) uplifted by movement on the fault, so that maintaining a course through them requires the rivers to incise or to keep their basins filled with sediment, which they will only do if their catchment is sufficient. Some gorges become abandoned and are left as dry valleys (Fig. 6), while the drainage that used to flow through them is either forced to find another outlet or ends in a closed basin. These developments are all accompanied by a strike-slip motion so that the rivers in the west can, in principle, find new outlets across the Abbarik mountains as they are moved north by the right-lateral component.

It is because the Abbarik mountains offer a barrier to the drainage from the west, with only a few outlets across it, that it is possible to unravel the drainage history and structure of the Gowk fault. As we will see, such an approach is not possible on the Nayband and Sabzevaran faults to the

Fig. 5. (a) View south from approximately position B in Fig. 7a across heavily incised alluvial surfaces grading towards the cultivated Joshan depression to the left of the photo. (b) View looking south along the scarps developed in Quaternary alluvium at Chahar Farsakh (see Fig. 9). (c) View northwest towards the Gowk fault scarp near Sarvestan (Fig. 3). The road can be seen climbing up the scarp, which is no more than 20 m high and interrupts an otherwise flat plain. (d) View north of the North Khanekhatun playa (white area to right) and incised fans cut by fault (centre). The fans grade eastwards (from left to right) and are incised by eastward flowing drainage. Note that dry valleys are developed east of North Khanekhatun (Fig. 6e–g), but Holocene scarps (marked f) show clear up-to-the-east movement through fans west of the main range front (black cross marks the upthrown side). (e) View southwards from Hashtadan towards the steep and incised northern slope of fans that separate this depression from Fandoqa (Figs. 10 and 12a). (f) View from the top of the Gaznau river fans looking south down the gentle south-facing alluvial surface towards Golbaf (Figs. 10 and 12a). (g) View looking eastwards towards the nose of the Shahdad blind thrust at 30°19′N 57°46′E (Fig. 3). A river has incised through the alluvium uplifted in the anticline. (h) Close-up view of the northern wall of the canyon in Fig. 5g. Small thrust faults are seen to cut through the uplifted alluvium.

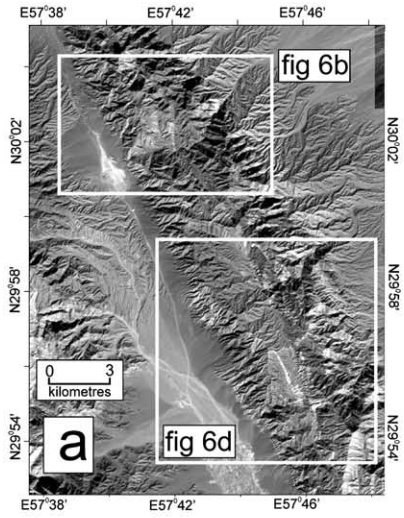
E57°38'
E57°42'
E57°46'
N30°02'
N29°58'
N29°54'
fig 6b
fig 6d
0 3
kilometres
a

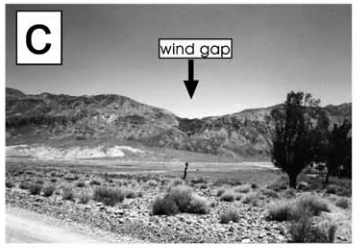
c
wind gap

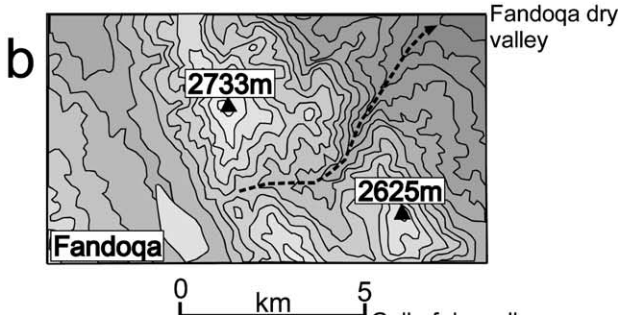
b
Fandoqa dry valley
2733m
2625m
Fandoqa
0 km 5

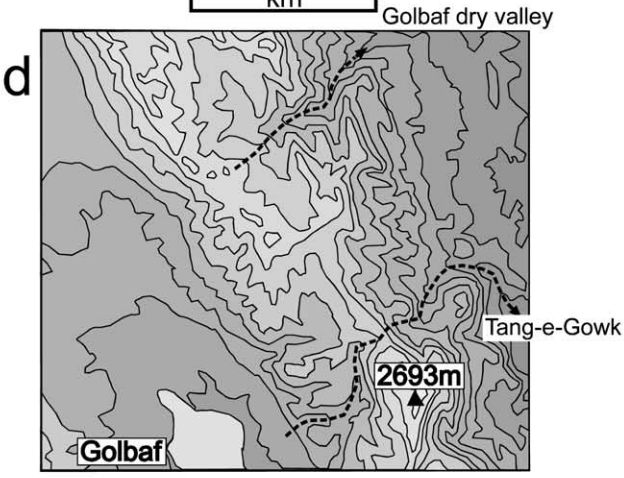
d
Golbaf dry valley
Tang-e-Gowk
2693m
Golbaf

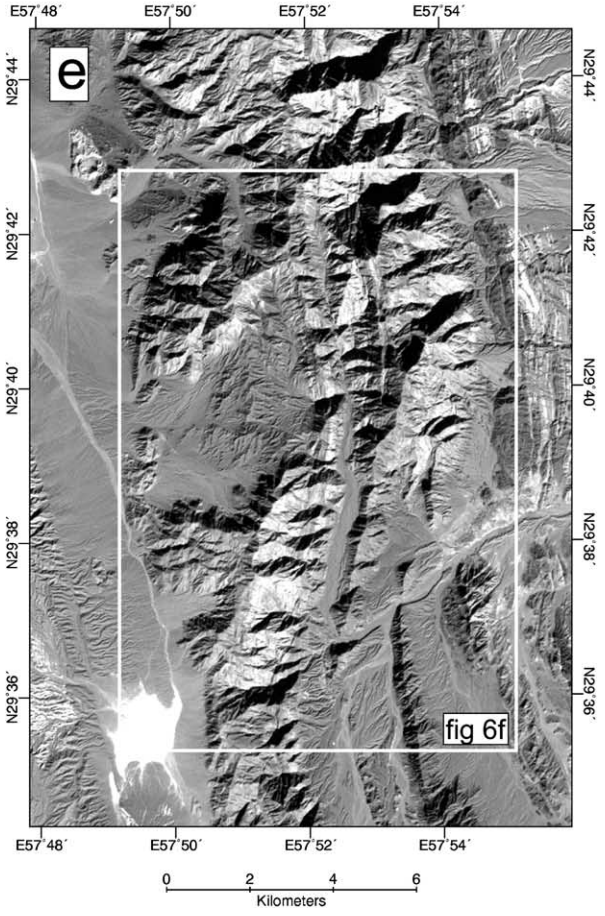
E57°48'
E57°50'
E57°52'
E57°54'
N29°44'
N29°42'
N29°40'
N29°38'
N29°36'
e
fig 6f
0 2 4 6
Kilometers

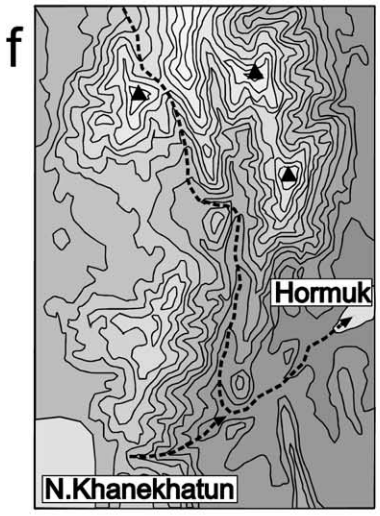
f
Hormuk
N.Khanekhatun
0 km 5

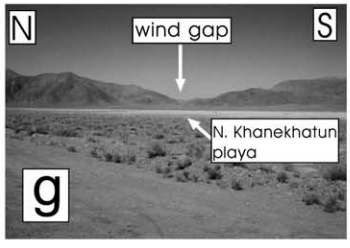
N
S
wind gap
N. Khanekhatun playa
g

north and south, where the drainage has an unimpeded crossing to the floor of the Lut.

3. Estimating offsets on the Gowk fault using drainage

3.1. Reconstruction of a 3 km offset

Fig. 7a shows the major drainage in the region around Sirch and Joshan. The Sirch river (S) exactly follows the fault for 2.9 km along a narrow linear gorge before crossing the fault and passing through the Abbarik mountains in the Sirch gorge at (1). The present-day Joshan river (J) also flows through the Sirch gorge, entering through a southern entrance via a large U-shaped bend, which lies to the east of the fault (3). The Hashtadan river (H) flows through the Hashtadan gorge (4) making an apparent (and, as we shall see, misleading) left-lateral step in its course at the entrance. There are numerous abandoned river channels and incised alluvial surfaces in this region (Fig. 5a). Joshan and Hashtadan villages occupy a cultivated depression about 5×2 km, elongated parallel to the fault. This depression is likely to be a pull-apart basin, caused by the right-stepping pattern of faults between the region south of the Hashtadan river and the Sirch gorges at (1) and (2). The pattern of the drainage and its associated fans can be used to demonstrate a right-lateral offset of 2.9 km in this region, shown in Fig. 7c. The main characteristics of the reconstruction and the geomorphic development we infer from it are:

1. The 2.9 km reconstruction (Fig. 7c) brings the outlet of the Sirch river in line with the entrance to gorge (1). The narrow ribbon of cultivation extending westwards from Joshan village is brought into a position adjacent to the present Hashtadan gorge (4). Note that the present-day Joshan river channel takes a more northward course incising through this cultivated zone, which lies on higher fluvial gravels. Stream A is now adjacent to the gorge at (3).
2. At the time of this 2.9 km reconstruction streams C and D were far from any of the four gorge outlets but were near the centre of the subsiding area caused by the local extensional component. So it is possible that, at least for a time, the Joshan depression was internally draining. The old fans formed by streams C and D (now incised) grade into the cultivated (and now also incised) floor of the Joshan depression (Fig. 5a).
3. At some time more recent than that represented by Fig. 7c the drainage reorganised. The Joshan river switched from the Hastadan gorge (4) to the northern gorge at (3), incising through the old fan systems and lowering the base levels to which the fans from streams C and D were graded (Fig. 5a). This capture of the Joshan river was aided by two processes. First, the northern gorges 1 to 3 are lower (~1500 m) than the Hashtadan gorge (~1600 m). Second, as the Joshan river was displaced north by the strike-slip motion its gradient within the Joshan depression was reduced, along with its ability to incise and keep its outlet to the Hashtadan gorge open. At the same time it became closer and more vulnerable to aggressive headward erosion by streams that could cut through the soft sediments of the depression to reach gorge 3. In order for the Hashtadan gorge (4) to remain open to the present day, it must have captured drainage from the Hashtadan river very soon after losing the Joshan river, so that vertical movement on the fault would not block the entrance to the gorge (as at Fandoqa, for instance; Fig. 6a–c).
4. An intermediate reconstruction with an offset of 0.6 km is shown in Fig. 7b. At this time stream A is adjacent to gorge 1 while stream B represents a new channel cutting through the old fan system to reach the entrance of gorge 2. We do not know whether by this time the outlets of streams C, D and the Joshan river had also switched to the north (3), but the course of the Joshan river is shown by the dashed line to illustrate the process.
5. The switching of the Joshan river to the lower gorge in the north has caused the incision of all drainage in the northern part of the basin, associated with streams B, C and D. It is evident that this switching was the decisive event from the lack of any incision in fans or the rest of the basin SE of the Joshan river.

The example of the Joshan depression provides evidence for a 3 km offset on the Gowk fault as well as an illustration of what happens when a river switches from one outlet across the Abbarik mountains to the next as a result of strike-slip movement. But when we look at the whole length of the Gowk fault, it is clear that this 3 km offset does not restore the drainage everywhere (Fig. 8b). Not only are there still large apparent offsets in the drainage at some places, such as Khanekhatun (stream 12 in Fig. 8b) but, more importantly, there are several dry valleys across the Abbarik mountains that have no obvious drainage entering them. Indeed, there is nothing very special about the offset of 3 km at Joshan, except that this is the obvious offset of the Sirch river at gorge 1 in Fig. 7.

Fig. 6. Evidence for dry valleys (wind gaps) crossing the Abbarik mountains and representing former water courses. (a) LANDSAT 7 image showing the Abbarik mountains adjacent to Fandoqa (see Fig. 3). Boxes show locations of (b) and (d). (b) Topographic map showing the Fandoqa dry valley which is now uplifted above the valley floor. (c) View east from Fandoqa showing the wind gap in the Abbarik range front representing the Fandoqa dry valley in (b). (d) Topographic map of the Tang-e-Gowk and Golbaf dry valleys. (e) LANDSAT 7 image of north Khanekhatun (see Fig. 3). Box shows location of (f). (f) Topographic map of the Hormuk dry valley. (g) View east from North Khanekhatun of the wind gap marking the Hormuk dry valley. (All topographic maps have 100 m contour intervals.)

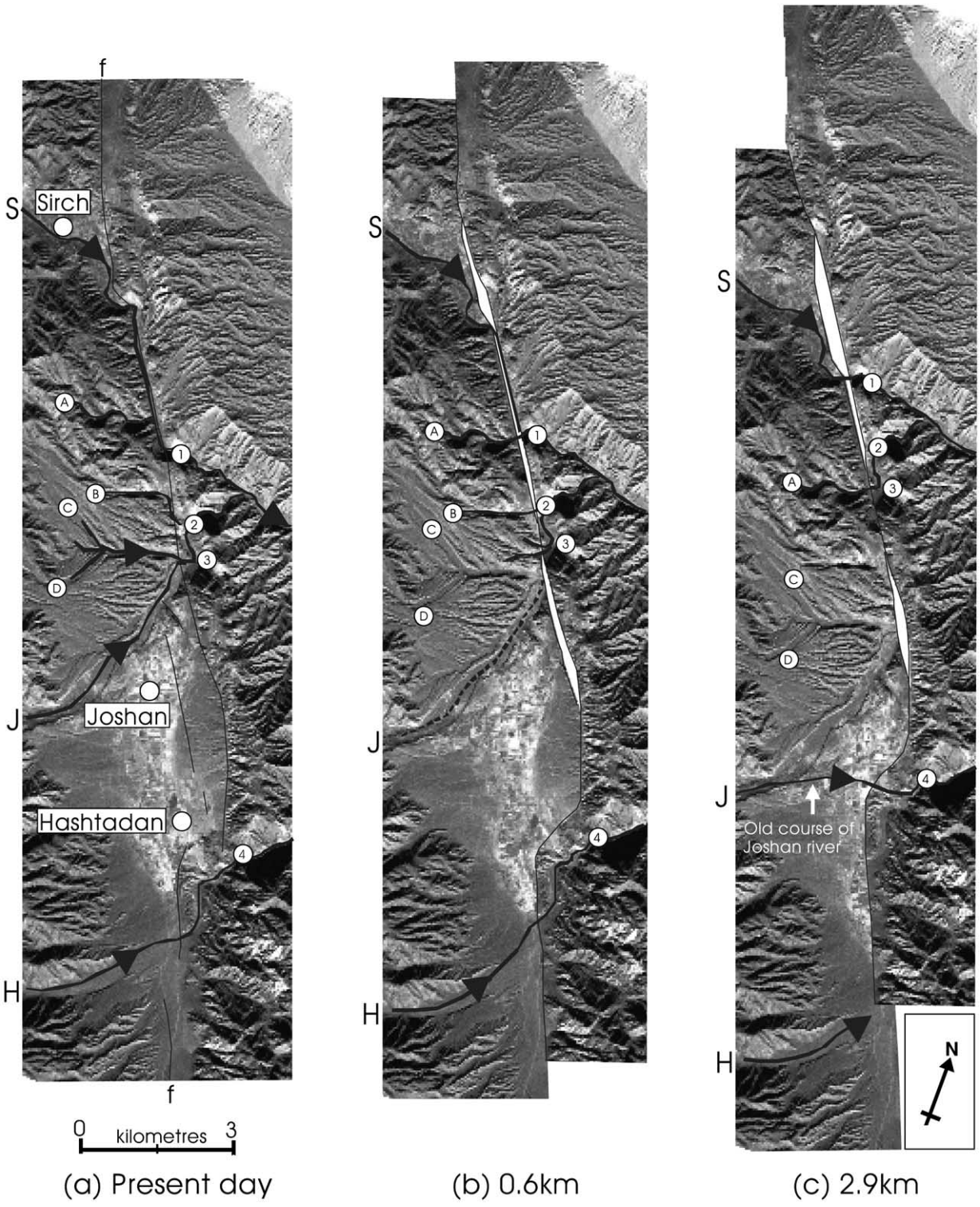

Fig. 7. Reconstruction of 3 km of fault movement at Sirch and Joshan (see Fig. 3 for location). (a) The present-day drainage. Both the Sirch (S) and Joshan (J) rivers drain into the Sirch gorge through outlets 1, 2 and 3. The Hashtadan river (H) drains through outlet 4. (b) With 0.6 km of dextral movement restored, streams A and B are adjacent to 1 and 2. The course of the Joshan river is uncertain at this time and so is dashed. (c) 2.9 km of restoration brings both the Sirch and Joshan rivers into line with gorges 1 and 4 and represents the probable drainage configuration at this point in the fault history. The apparent left-lateral deflection of the Joshan river in (a) is thus a product of stream capture. The process of stream capture has caused deep incision of alluvial surfaces north of Joshan (Fig. 5a) as streams adjust to the new base-level (see text for detailed explanation).

3.2. Evidence for a 12 km offset

Fig. 8c shows a reconstruction of a 12 km offset on the Gowk fault. In this reconstruction most of the rivers draining the Sekonj mountains in the west are now adjacent to present-day gorges or dry valleys in the Abbarik mountains in the east. In addition, the courses of most rivers are now much straighter, particularly for the streams with apparently large offsets in Fig. 8a, such as streams 7 (the Gaznau river) and 12 (the Khanekhatun river). Those two streams, which today flow longitudinally for ~15 and ~12 km parallel to the fault before finding their present-day exit across the Abbarik mountains, flow past several dry valleys on the eastern side of the valley (Figs. 6 and 8a). The implication is that, early on, these dry valleys were unable to maintain their gorges through the mountains and so were abandoned.

Not all the streams and dry valleys are matched by the reconstruction in Fig. 8c. Streams 9 and 10 have no apparent outlet, but this may be because the preservation of their initial courses through the Abbarik mountains is too subtle to be seen. The two dry valleys south of Hormuk (opposite stream 12 in Fig. 8a) are apparently unused in Fig. 8c. However, in this case it is clear that the drainage patterns west of the fault have been altered, with present-day streams flowing south to join the main course of stream 12 cutting through large alluvial fan systems that once graded to the east (Fig. 5d). We suspect that the original streams flowed east but, once the gorges in the east were abandoned as dry valleys, they were captured by streams to the south.

There is further independent evidence to support the 12 km reconstruction. Restoration of the fault by this amount removes the depression at Chahar Farsakh (Fig. 3, discussed later), which is in a pull-apart location in a right-step between the southern end of the Nayband fault and the Gowk fault. An offset of 12 km restores the northern end of the Abbarik mountains into continuity with the western side of the Nayband fault and also puts the northern end of the Shahdad anticline adjacent to the southern terminus of the Nayband fault (Fig. 8c). Although no lithological offsets can be demonstrated across the fault due to the differing geology of the Sekonj and Abbarik mountains, there is an abrupt change in the colour of the alluvial deposits as seen on LANDSAT imagery (S–S′ in Fig. 3; see also "Electronic Supplements" on the journal's homepage: http://www.elsevier.com/locate/jstrugeo for a more detailed image). This change presumably relates to the different provenances, with Cretaceous limestones exposed in the mountains east of Khanekhatun and volcanic rocks in the Jebal Barez mountains to the south. A 12 km restoration of this offset aligns these changes either side of the fault. Finally, an offset of 12 km restores the northern margin of the Jebal Barez mountains at the southern end of the fault along line R–R′ in Fig. 3.

Thus, restoration of a 12 km offset on the Gowk fault produces a situation in which there is much greater continuity in the topography and drainage than is seen today, with rivers crossing the line of the Gowk valley from the Sekonj mountains, through the Abbarik mountains to the Dasht-e-Lut. Indeed, there is no reason to suppose that the Gowk valley existed at all at the time represented by this restoration. It appears to us, therefore, that 12 km is likely to be the total strike-slip offset on the Gowk fault: any attempt to restore more than that would require a complete re-arrangement of the topography and drainage, not only of the Abbarik–Sekonj–Nayband mountains, but of the Jebal Barez range front as well. The position of the Gowk fault itself may well be related to the fact that the older rocks of the Sekonj and Abbarik mountains are quite distinct: they were perhaps separated by an older thrust fault that became reactivated in a strike-slip sense when the Nayband–Gowk system became active. We discuss the timing of this 12 km offset on the Gowk fault later.

4. Development and structure of the Gowk fault system

So far we have used the geomorphology to estimate the offset on the Gowk fault. In this section we use it to investigate the fault structure at depth and how the faulting evolves with time. The strike-slip component of motion largely determines the longitudinal evolution of the Gowk valley, while the structure at depth is reflected mainly in the vertical motions at the surface.

4.1. Longitudinal structure and evolution of the fault zone

4.1.1. The northern end: Chahar Farsakh to Sirch

The northern end of the Gowk fault and the southern end of the Nayband fault form a right-stepping overlap near Chahar Farsakh (Figs. 3 and 9). In this stepping arrangement, a local extensional component is expected (Fig. 9c), and the overlap region between the faults is one of subdued relief and low elevation. Only isolated scarps and fault traces are visible in the overlap region as the majority of geomorphic features have been eradicated by the large drainage catchment that is focused into this basin from the mountains to the north, west and south. The Shahdad river cuts a deep gorge through the basin as it flows unimpeded to the Dasht-e-Lut and has left abandoned uplifted terraces on the west side of the fault at Chahar Farsakh. No right-lateral offsets are seen where this river crosses either of the two fault strands in Fig. 9b, probably because of the locally high rate of fluvial activity. The scarp at Chahar Farsakh, which is about 60 m high (Fig. 5b), and the uplifted flat terraces on the west side are consistent with a down-to-the-east normal component of motion on the roughly N–S fault, which is expected in this location.

The Chahar Farsakh basin thus accumulates sediment because of its pull-apart configuration. But, with continued right-lateral movement on the Gowk and Nayband faults, material that was originally deposited in the Chahar Farsakh depression will enter a zone with a shortening component

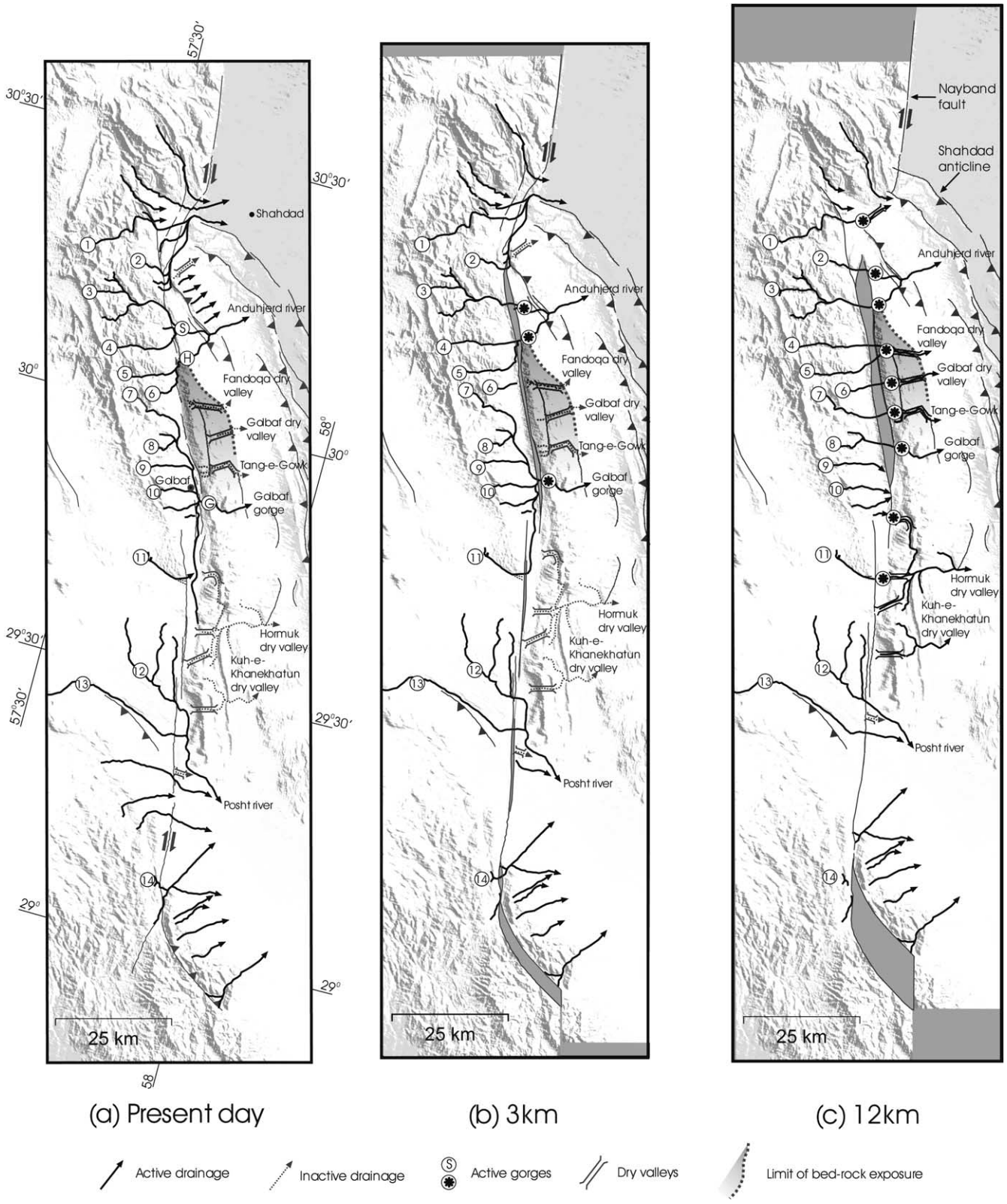

because the strike of the Gowk fault (155°) is oblique to the regional slip vector (~175°) (Fig. 9c). This shortening causes the newly-deposited sediments to be uplifted and eroded as they move south, and has an important influence on the structure and morphology on the eastern side of the Gowk fault. North of Hashtadan (Fig. 7a) the eastern side of the Gowk fault is composed of Quaternary alluvium at the surface, whereas farther south lithified Cretaceous sediments are exposed (this transition is marked by the dashed line in Fig. 8, separating grey lithified rocks to

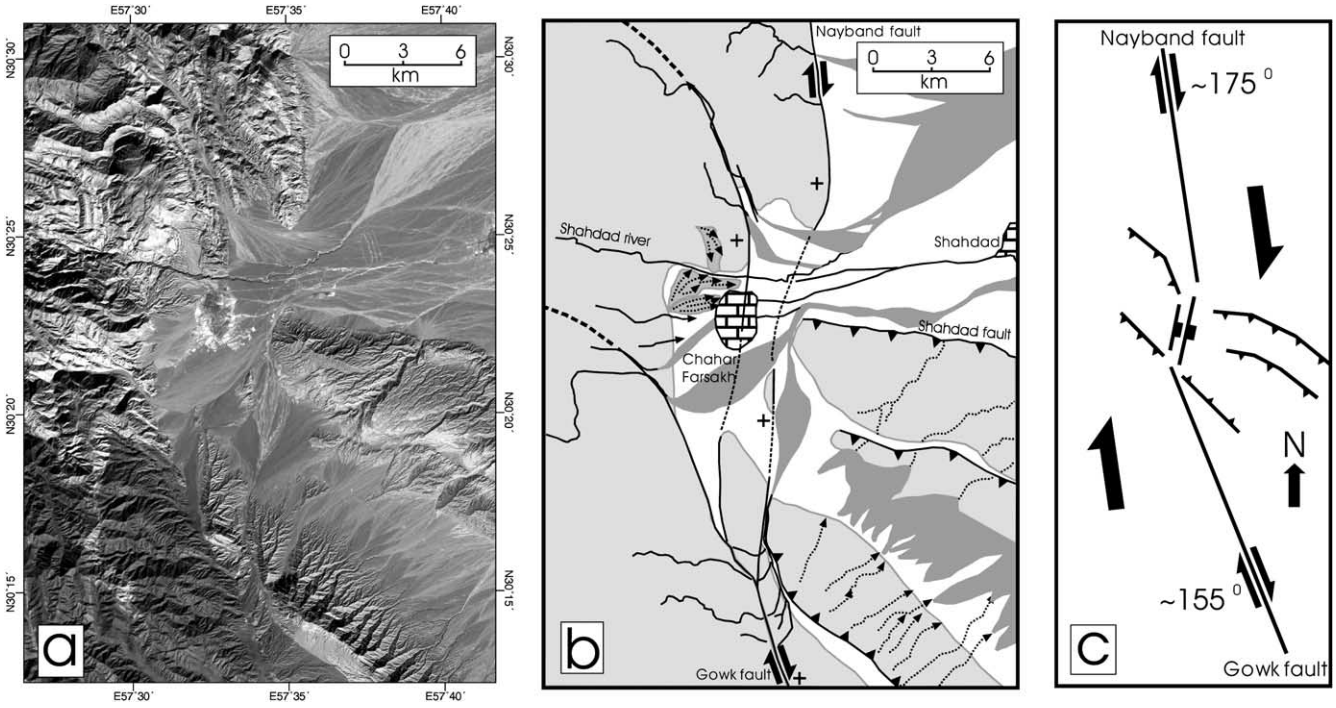

Fig. 9. (a) LANDSAT 7 view of the Chahar Farsakh pull-apart depression (Fig. 3 for location). (b) Geomorphic map of the same region. High ground is marked in light grey, alluvial fans in dark grey. Drainage is focused towards the low ground of the depression. (c) Schematic sketch of the Chahar Farsakh region. Local extension is expected in the region between the Nayband and Gowk faults. Assuming the regional slip vector is parallel to the Nayband fault (~175°), material that is first deposited in the pull-apart depression will later be subjected to shortening and uplift as it is moved to the SSE along the Gowk fault.

the south from alluvium to the north). This contrast in the hardness of the rocks is reflected in the drainage: to the south are numerous abandoned dry valleys (as at Fandoqa and Golbaf; see Fig. 6), but north of Hashtadan downcutting of streams through the fault has generally managed to keep pace with the uplift. Continued uplift to the east will eventually expose bed rock beneath the Quaternary sediments in the north which will be much harder to erode. This, in turn, will cause a transition to a morphology more like that seen at Fandoqa and Golbaf, with dry valleys and longitudinally displaced rivers flowing along the valley. The section between Chahar Farsakh and Fandoqa thus preserves different stages in the development of the fault and its drainage.

4.1.2. The central section: Khanekhatun to Sirch

The central part of the Gowk fault, from Khanekhatun to Sirch (Figs. 3 and 10), is a series of cultivated basins separated by local highs with relief of up to 400 m. The highs are composed of incised Quaternary alluvial fans deposited by rivers flowing into the valley from the Sekonj mountains to the west. However, these topographic highs are not always barriers to the present-day longitudinal drainage, which in some cases has incised deeply through the barrier to reach a sink at the other side. A topographic profile along the valley, entirely within the alluvial deposits, shows an asymmetric saw-tooth pattern in the northern part, with steeper slopes to the north and gentler slopes to the south (Fig. 10). Fig. 10 emphasizes that not all the depressions have active outlets (filled circles) through the Abbarik mountains. Some (open circles), such as at Fandoqa, are now adjacent to uplifted and abandoned dry valleys. The longitudinal drainage directions are shown by arrows indicating, for example, that drainage from North Khanekatun pierces two topographic highs to reach the gorge at Golbaf. The asymmetry of the longitudinal profile dominates the appearance of the valley in the field (Fig. 5e and f), but since it does not control the drainage, the drainage must

Fig. 8. (a) Present-day drainage across the Gowk fault. Active gorges through the Abbarik mountains (east of the fault) are developed at Sirch (S), Hashtadan (H) and Golbaf (G) and are marked with black stars in (b) and (c). The northern limit of bed-rock exposure east of the fault is marked by the dark-grey shaded area. Two of the three active gorges (S and H) are developed in Quaternary alluvium north of this. Note the large apparent dextral offsets of streams 7 and 12. Abandoned drainage systems east of the fault are shown as grey dotted lines. (b) Restoration of 3 km of dextral movement as demonstrated in Fig. 7. Although streams 3 and 4 are adjacent to outlets, the majority of the drainage still shows large apparent offsets (e.g. streams 5, 7, 11 and 12), and several dry valleys have no obvious catchments. (c) 12 km of dextral movement restores the majority of the drainage to simple linear patterns, with most streams now adjacent to active gorges or dry valleys. This reconstruction brings the Shahdad thrusts into line with the southern tip of the Nayband fault and also fills in the Chahar Farsakh pull-apart at the north end of the fault placing the present-day region in which Quaternary alluvium is exposed east of the fault (north of the shaded area) within the pull-apart.

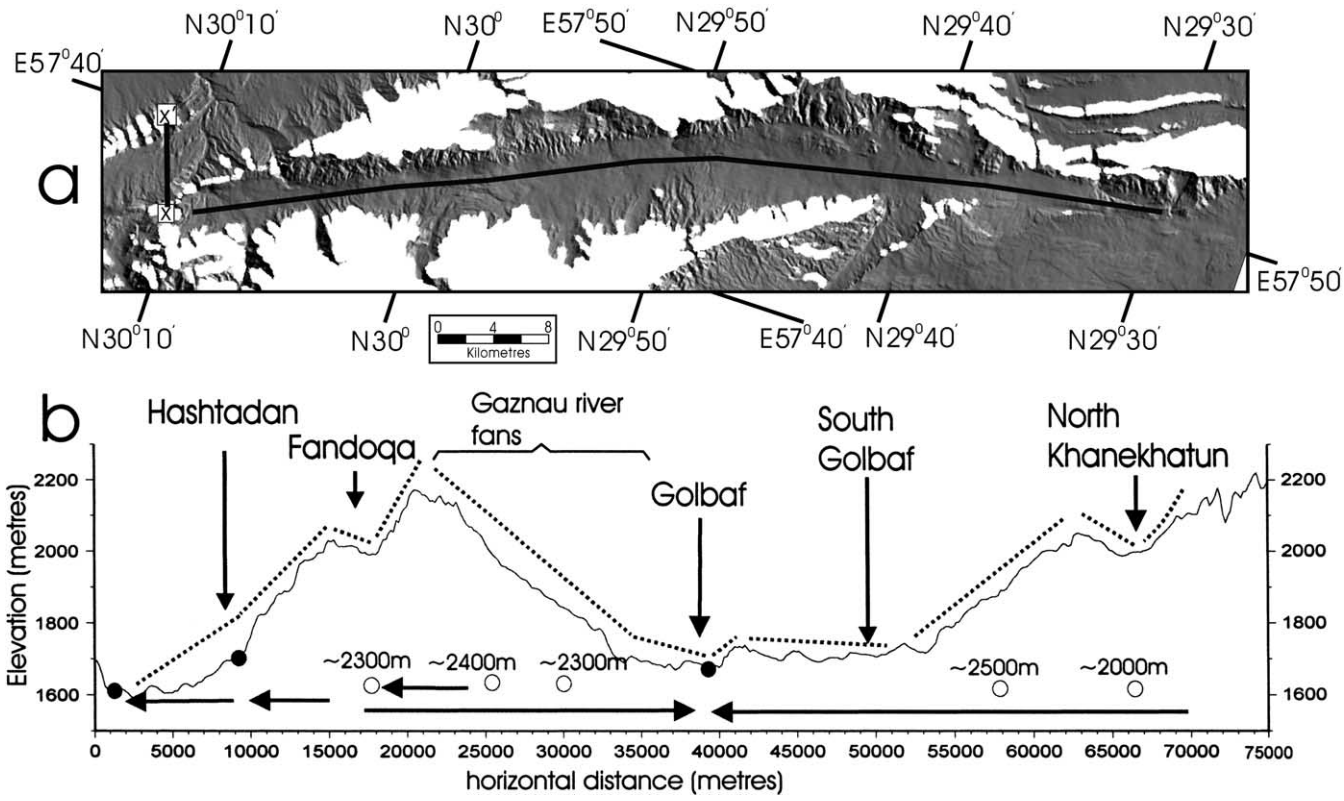

Fig. 10. (a) A 40 m resolution digital elevation model of the Golbaf valley from Sirch in the north to North Khanekhatun in the south. The N–S line represents the line of section shown in (b). The short line X–X′ at the top of the diagram represents the line of section in Fig. 13. (b) Topographic profile taken from the 40 m resolution digital elevation model along the axis of the Golbaf valley. Active gorges through the Abbarik mountains (east of the Gowk fault) are marked with filled circles. Positions of dry valleys within the Abbarik mountains are marked by open circles, and the heights above sea-level of their present-day drainage divides or wind gaps are shown above them in metres. Arrows along the base of the profile show drainage directions along the valley axis. A saw-tooth pattern of steep north-facing slopes and gentle south-facing slopes is seen in the northern half of the profile, which has probably developed in the manner described in Fig. 11. Note that the drainage directions do not necessarily follow the topographic gradients on the fan surfaces.

have changed with time. The way it may have done so is illustrated in Fig. 11:

1. Right-lateral movement on the fault displaces the rivers longitudinally, progressively increasing their length and reducing their gradient, causing them to aggrade (Fig. 11b).
2. Uplift east of the fault raises the level of the outlet with respect to the fluvial base-level in the valley, also encouraging sediment accumulation in the basin and also reducing the stream gradient west of the fault (Fig. 11b).
3. Continued right-lateral offset will eventually bring the river close to a more northerly outlet or sink (Fig. 11c). If it is captured by a stream draining north, the sudden drop in base-level to the new and closer gorge causes deep incision through the northern part of the fan, resulting in steep, incised north-facing slopes compared with the smoother and more gentle south-facing slopes.

Two examples illustrate this process. The first is the Gaznau river (stream 7 in Fig. 8), whose outlet is currently at the Golbaf gorge (Fig. 12). When the Gowk fault was initiated (Fig. 8c), the Gaznau river would have been adjacent to a different outlet, the Tang-e-Gowk dry valley. Flow through that outlet was evidently insufficient to overcome up-to-the-east movement on the fault and the Gaznau river was deflected longitudinally to exit through the Golbaf gorge, which was originally occupied by the Zamanabad river (stream 8 in Fig. 8). Continued right-lateral offset and subsidence west of the fault has acted to flatten the stream profile and fill the Golbaf depression with sediment. The head of the Gaznau fan is now almost adjacent to Fandoqa, but there is no longer an outlet at Fandoqa, as that has also been uplifted and abandoned to leave a dry valley. So the Gaznau river still flows south, resulting in an extremely elongate river profile of low gradient. Meanwhile the older, inactive parts of the Gaznau fan, which once drained east near 30°N, have been captured and incised by streams flowing into the now-internally draining Fandoqa depression.

A second example is the drainage flowing north from North Khanekhatun to the Golbaf gorge (Fig. 12b), incising through topographic highs (Fig. 10). When the Gowk fault was initiated, the Neybid river (stream 11 in Fig. 8) would have flowed through the now uplifted and abandoned valley

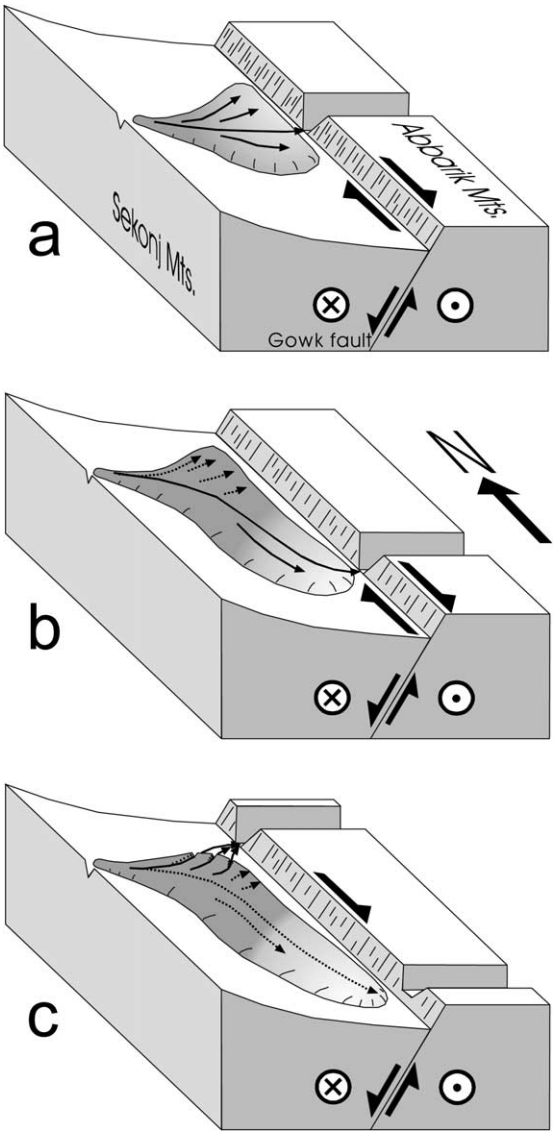

Fig. 11. Schematic development of the longitudinal valley topography shown in Fig. 10. (a) A river draining eastwards from the Sekonj mountains develops a gorge through the uplifting Abbarik mountains. (b) Continued right-lateral movement displaces the river longitudinally, increasing its length, reducing its gradient, and encouraging sediment accumulation in the basin. Active river channels are deflected southwards leaving inactive eastward-facing channels. (c) If continued right-lateral movement brings a more northerly gorge (or deep, internally-draining basin) into line with the river, drainage from that gorge or basin may capture the river. The sudden drop in base-level will cause rapid incision of the north-facing slope (as at Joshan; Fig. 5a).

east of North Khanekhatun which leads to the village of Hormuk (Fig. 8c). As right-lateral faulting displaced the western part of the river to the north, the Hormuk gorge was uplifted and abandoned, possibly aided by the capture of the Neybid river by streams draining to the South Golbaf depression, which occupies a pull-apart position in a right-step between two major fault segments (Fig. 12b). The subsiding South Golbaf depression also receives catchment from mountains to both the east and west but is no longer internally draining as it has in turn been captured by the streams draining north to the even lower Golbaf gorge. The South Golbaf depression is filled with clay beds that must be older than the link to the Golbaf gorge and are now deeply incised by the through-going longitudinal drainage. Once again, it is the northern end of the south Golbaf depression that is incised following capture by the next basin to the north (as the old Gaznau fans were captured by the Fandoqa depression in Fig. 12a).

4.1.3. The southern end: Khanekhatun to Jebal Barez

The southern part of the Gowk fault, from Khanekhatun through Sarvestan to the Jebal Barez mountains is very simple, with a single east-facing scarp of ~20 m height for much of its length (Fig. 5c). The scarp cuts a plain that slopes gently eastwards and is not associated with any other topography. This is no surprise as the trend of the fault in this section returns to the (probable) slip vector direction of ~175° seen on the Nayband and Sabzevaran faults, and the restraining orientation of the central Gowk fault is lost. The Shahdad anticline system in the east also ends in the south at the latitude of North Khanekhatun (Fig. 3), reflecting this change in strike.

4.2. Dip-slip movements and the structure at depth

From a study of the 1981 and 1998 earthquakes in the Gowk valley, Berberian et al. (2001) proposed that, in cross-section, the Gowk fault system resembles a ramp-and-flat geometry on which there is both thrust and strike-slip motion, shown schematically in Fig. 4a. The geometry in Fig. 4a has various consequences for the longer-term vertical motions expected in the vicinity of the faulting, which we examine in this section.

There is abundant evidence that the Abbarik mountains have been uplifted relative to the Gowk valley. South of Sirch are numerous dry valleys marking the sites of uplifted and abandoned gorges that once crossed the Abbarik range, now up to 800 m above the valley floor (Fig. 10). Near Sirch itself, where the east side of the valley is mostly alluvial deposits rather than Cretaceous rocks, relative uplift of at least 350 m can be demonstrated by preserved tilted alluvial surfaces that are now separated from their drainage source to the west (Figs. 7a and 13).

In principle, these estimates of the relative uplift across the Gowk valley indicate the minimum height of the postulated 'ramp' beneath the Abbarik mountains. Within the Gowk valley itself there are east-facing scarps, some of which were reactivated at the surface in 1981 and 1998. These all cut through Quaternary alluvial fans, occurring never more than 100 m west of parallel west-facing scarps. They appear to be near-surface expressions, in the manner shown in Fig. 4d, of tensional failure where the rupture passes through unconsolidated alluvial deposits, rather than to be representative of faulting at depth.

There is also evidence that the area east of the Abbarik

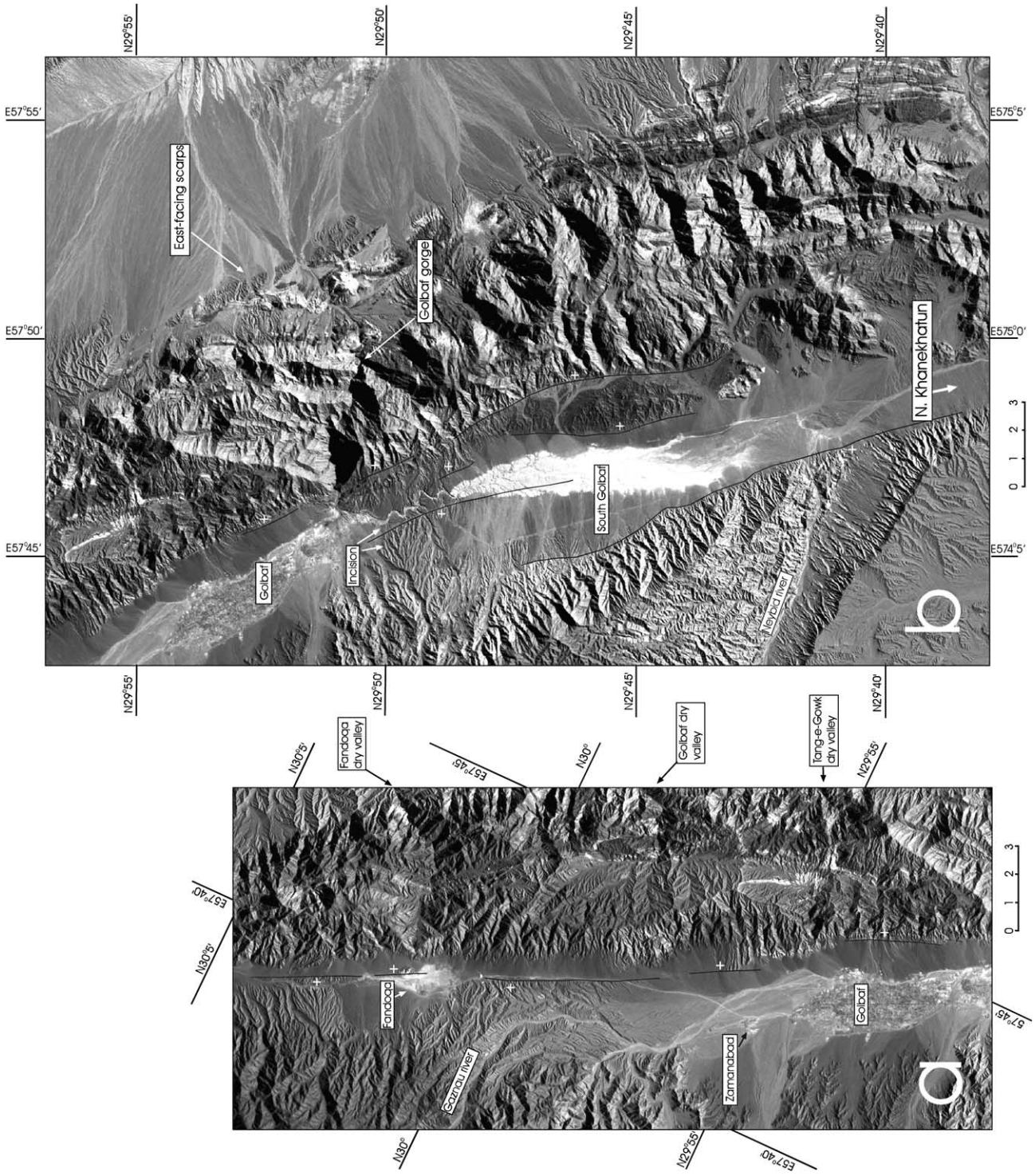
East-facing scarps
Golbaf gorge
Golbaf
Incision
South Golbaf
Sirjod river
N. Khanekhatun
b
Fandaqa dry valley
Golbaf dry valley
Tang-e-Gowk dry valley
Fandaqa
Gezmaou river
Zamanabad
Golbaf
a
N29°55'
N29°50'
N29°45'
N29°40'
E57°55'
E57°50'
E57°45'
E575°5'
E575°0'
E574°5'
N30°5'
N30°
N29°55'
E57°40'
E57°45'
0 1 2 3

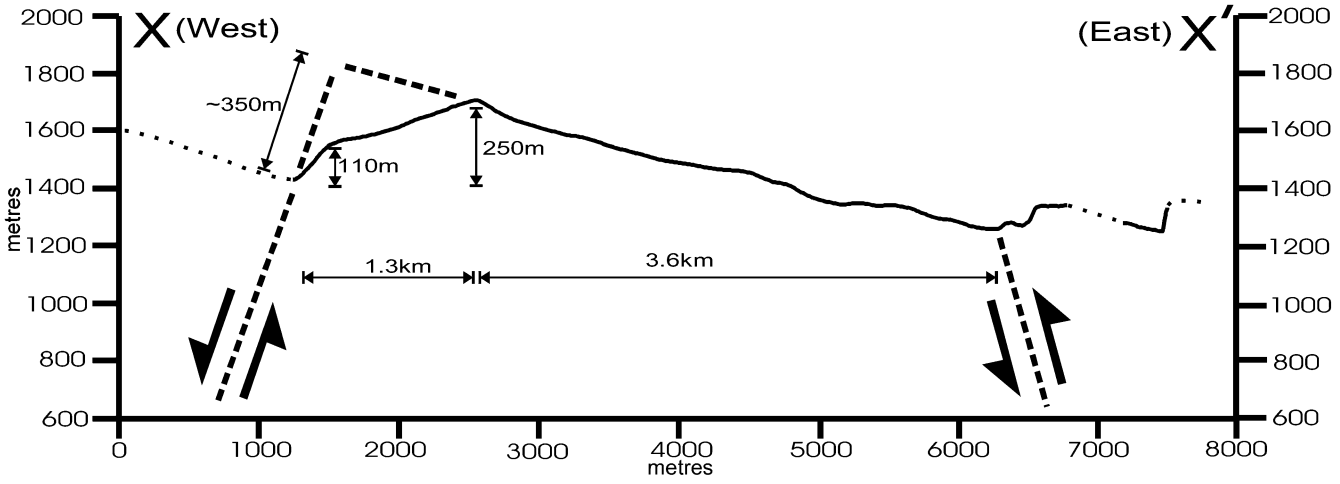

Fig. 13. Profile across the Gowk fault south of Sirch, taken from 40 m DEM. Dotted sections represent areas without data coverage. The line of profile is marked on Fig. 10a. A minimum of 350 m of dip-slip fault movement can be demonstrated from the uplift of Quaternary alluvium, which defines a gently eastward-dipping surface.

mountains is uplifting relative to the Dasht-e-Lut, as all the streams that cross this region incise deeply through canyons. The uplift appears to occur in two places: on the steep eastern flank of the Abbarik mountains, and on the Shahdad fold-and-thrust system. Published geological maps (Aghanabati, 1993) mark faults along the eastern edge of the Abbarik mountains (the area is inaccessible in the field because of security considerations). On LANDSAT images they appear as linear east-facing scarps up to 150 m high, causing incision of their western sides (Fig. 12b). We interpret them as steep reverse faults within the Quaternary alluvial apron. Along-strike to the north these faults appear to become blind as the Quaternary alluvial sediments show increased folding and incision at the surface.

The Shahdad fold system forms a series of three or four arcuate sub-parallel rows of anticlines, roughly parallel to the trend of the Abbarik mountains. Only the frontal anticline is accessible in the field, near Shahdad, but this is enough to infer the general structure of the ridges, which are formed of uplifted alluvial and playa deposits. The ridges are asymmetric, having dips of up to 30°NE on their eastern flanks, and much gentler dips of typically 5° on their western sides. Where one river gorge crosses the frontal anticline, small SW-dipping thrusts can be seen in the alluvial and uplifted river deposits (Fig. 5g and h). It seems safe to infer from the surface that the ridges are formed above blind thrusts, as deduced from radar interferometry by Berberian et al. (2001).

The drainage patterns allow us to make some inferences about the development of the Shahdad folds, as has been done elsewhere (Burbank et al., 1996; Jackson et al., 1996; Mueller and Talling, 1997; Bayasgalan et al., 1999b). Alluvial fans are produced at the exits to incised gorges through all the folds (Fig. 14). However, the fans associated with the inner series of folds are often abandoned, with the streams now incised in channels through the fan deposits, while the fans associated with the outer anticline are still active. This suggests that the eastern (frontal) folds are younger than those in the west, as is common in many fold-and-thrust belts.

Drainage courses are often deflected south around the ends of individual folds, with the deflection being greatest (up to 10 km) for courses across the innermost row of anticlines (Fig. 14). Rivers crossing the folds farther east show smaller or no lateral deflections. These deflections could be caused by fault-and-fold growth, with lateral propagation to the south (e.g. Jackson et al., 1996). The large catchments developed in this way by the innermost folds seem sufficient to maintain gorges through the outer folds without additional lateral deflection of stream courses.

The Shahdad folds die out in the south where the strike of the Gowk fault changes from ~155° back to the value of ~175° typical of the Nayband and Sabzevaran faults to either side (Fig. 3). The change of strike implies a loss of the shortening component on the Gowk fault, so this is no surprise. The shortening component in the central part of the Gowk fault must be taken up by the folds and thrusts east of the Abbarik mountains, and the amount of shortening is enhanced by any localised extension in the Gowk valley caused by the small extensional component there. If our reconstruction in Fig. 8c is correct, and if the overall slip vector across the system is ~175°, then 12 km of strike-slip

Fig. 12. (a) LANDSAT 7 image of the region between Fandoqa and Golbaf. (b) LANDSAT 7 image continuing (a) southwards to South Golbaf. Holocene scarps are shown as thin black lines, white crosses mark the upthrown sides (see Fig. 3 for locations). At the eastern edge of the mountains, clearly defined east-facing scarps can be seen. These scarps are developed in Quaternary alluvium and are up to 150 m high.

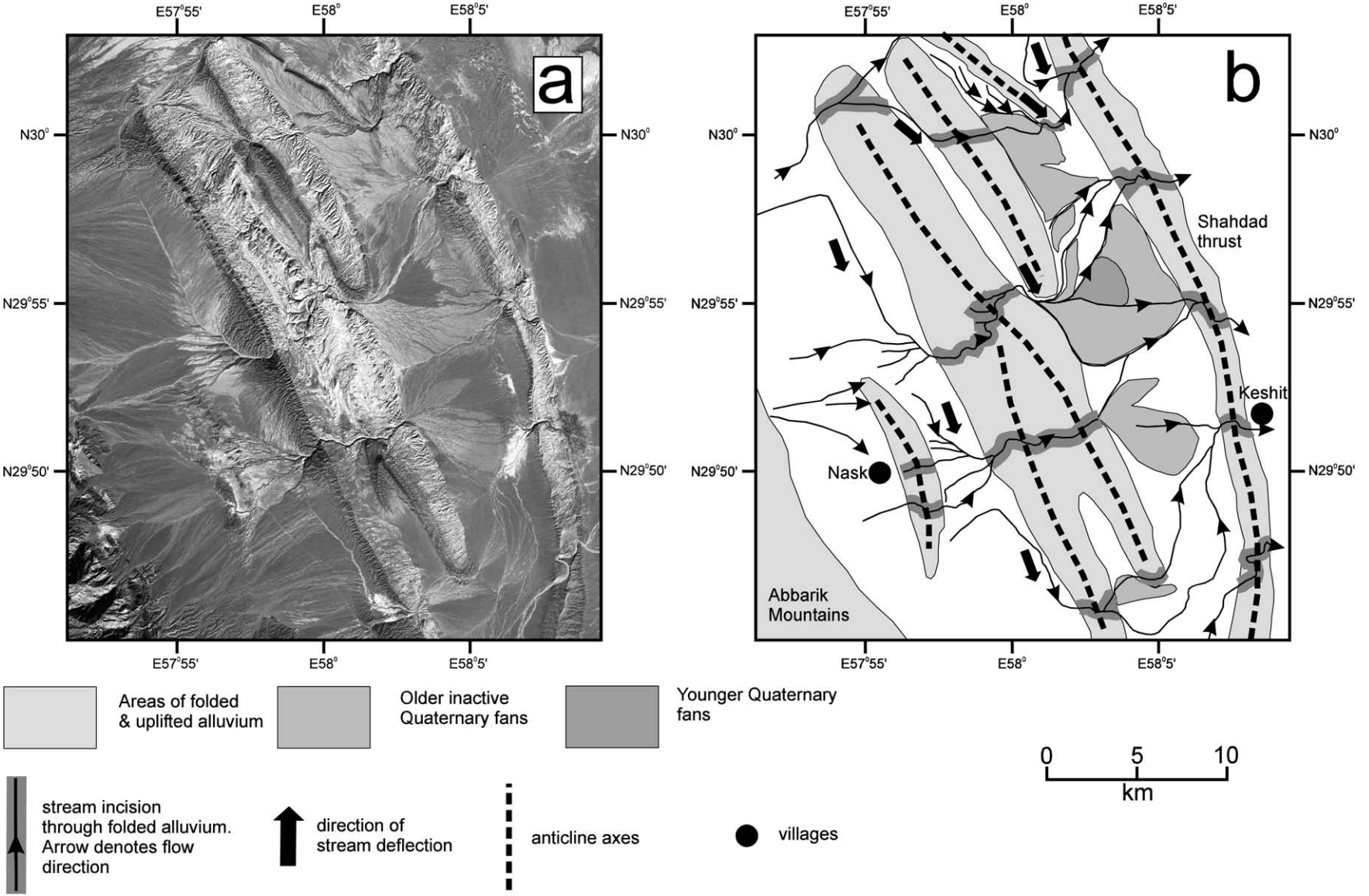

Fig. 14. (a) LANDSAT 7 image showing part of the Shahdad blind thrust system (see Fig. 3 for location). (b) Geomorphic map of the same region showing major drainage and preserved alluvial fans. Apparent southward drainage deflections are marked by black arrows. Abandoned alluvial fans are widely preserved at the exits to gorges through the inner series of folds.

faulting on the 155° trend of the central Gowk fault requires about 4 km of shortening perpendicular to the fault. We lack the detailed structural information needed to fully restore the folds, but they are clearly major structures, with dips of up to 30° on their eastern limbs, and are likely to be broken by thrust faulting at depth (Berberian et al., 2001). It is conceivable that they could accommodate 4 km or more of shortening on underlying blind thrusts.

The vertical motions we can see in the geomorphology are therefore compatible, in general, with the sub-surface geometry illustrated in Fig. 4a. But this configuration of faulting is inherently unstable for large amounts of slip on the lower thrust. As material moves up the ramp, the existing high-angle faulting in the Gowk valley and on the east side of the Abbarik mountains can no longer accommodate the change in dip on the underlying thrust. We would expect the faulting to migrate to the west in both places (Fig. 4b and c). We have examined the geomorphology and evidence for faulting on air photographs and satellite imagery, but can see no convincing evidence of such migration. There are places in the Gowk valley, at Joshan (Fig. 7a) and in north Khanekatun (Figs. 5d and 6e), where the most recent faulting appears to be within the valley and west of the fault forming the main linear range front, but we are not convinced that this is real evidence of the migration implied in Fig. 4b and c, as the faulting often steps to the right down the length of the valley anyway, as at Hashtadan in Fig. 7a and South Golbaf in Fig. 12b. Fig. 4b and c may be too simplistic a model of the fault evolution anyway, as adjustments could be made to the faulting at depth rather than at the surface.

5. Offsets on the Nayband fault and slip rates

There are no distinctive markers on the Gowk fault that can be dated to allow an estimate of slip rates. However, that opportunity is provided farther north on the Nayband fault, where Quaternary alkali basalts with lines of eruptive cones that follow the fault trace are offset in a right-lateral sense (Fig. 15). In this region the Rud-e-Shur river is offset 3.2 km, with drainage reorganisations also occurring at offsets of 0.65 and 2 km (Fig. 15c). Other stream displacements are noted from further north, some of which are described by Wellman (1966). Fig. 15b shows the Quaternary basalts of Gandom Berian, which have been cut by the Nayband fault, with an apparent offset of 3.2 km across the northern margin of the flows (Griffis, 1981). The course of the Rud-e-Shur river is younger than the basalt flows, having been deflected round them in the south, and is also offset 3.2 km. K–Ar dating of these volcanics yielded an age of 2.08 ± 0.07 Ma (Conrad et al., 1981). So since eruption of the basalt there has been a minimum of 3.2 km of right-lateral motion, giving a slip rate of ≥1.5 mm/year for the Nayband fault.

Slip on the Nayband fault is transferred in the south onto the Gowk fault along with any slip on the Kuh Banan fault to the west (Fig. 2b). At 1.5 mm/year, the 12 km offset on the Gowk fault could be achieved in 8 Ma, or less if there is some enhancement of this slip rate from the Kuh Banan fault. We conclude that most of the 12 km offset on the Gowk fault has been achieved since the reorganization of the tectonics of Iran ~5 Ma ago, as discussed in Section 2.1.

6. Implications for the active tectonics of eastern Iran

We have demonstrated that the probable offset on the Gowk fault section of the Nayband–Gowk–Sabzevaran system is about 12 km, most of it achieved over the last 5 Ma. Over that time interval we expect about 100–125 km of right-lateral shear to have occurred between central Iran and Afghanistan (Section 2.1). The implication is that most of this shear has happened on the east side of the Dasht-e-Lut on the fault systems of Sistan, an idea compatible with the observations of Freund (1970) and Tirrul et al. (1983) who estimate offsets of 13 and ~60 km on the Zahedan and Neh faults, respectively (Fig. 2). This is an important conclusion for the active tectonics of eastern Iran. At a latitude of 34°N the N–S right-lateral faulting changes to a system of E–W left-lateral faulting, which can only accommodate the N–S right-lateral shear if the faults rotate clockwise (Fig. 2b; Jackson and McKenzie 1984; Jackson et al., 1995). Since the N–S shear is faster on the east side of the Lut block than on the west, the E–W faults must rotate and bend more in the east than in the west. This appears to be the case with the Doruneh fault (Fig. 2b), which is relatively straight in the west but bends abruptly south in the east.

Thus we believe the slip rates on the fault systems east of the Lut are faster than those on the west. Both systems contain linear fault segments that exceed 100 km in length and are therefore capable of producing very large earthquakes of $M_w > 7.5$ (Berberian and Yeats, 1999). On the other hand, with slip rates of ~2 mm/year on the Nayband–Gowk system, the repeat time for events that slip ~5 m on faults 100 km long is likely to be in the order of 2000 years. There is no historical evidence for such large earthquakes on either side of the Lut in the last 2000 years (Ambraseys and Melville, 1982; Berberian and Yeats, 1999), but this is not conclusive, as the whole region is very isolated and relatively uninhabited. Earthquakes are likely to be more frequent on the Gowk fault, as it is relatively discontinuous with shorter fault segments that can accumulate less slip between events (e.g. Scholz, 1982), and indeed there is much more evidence of activity in the Gowk valley both recently and in the last few hundred years (Ambraseys and Melville, 1982; Berberian and Yeats, 1999).

7. Conclusions

We conclude that the total cumulative right-lateral offset

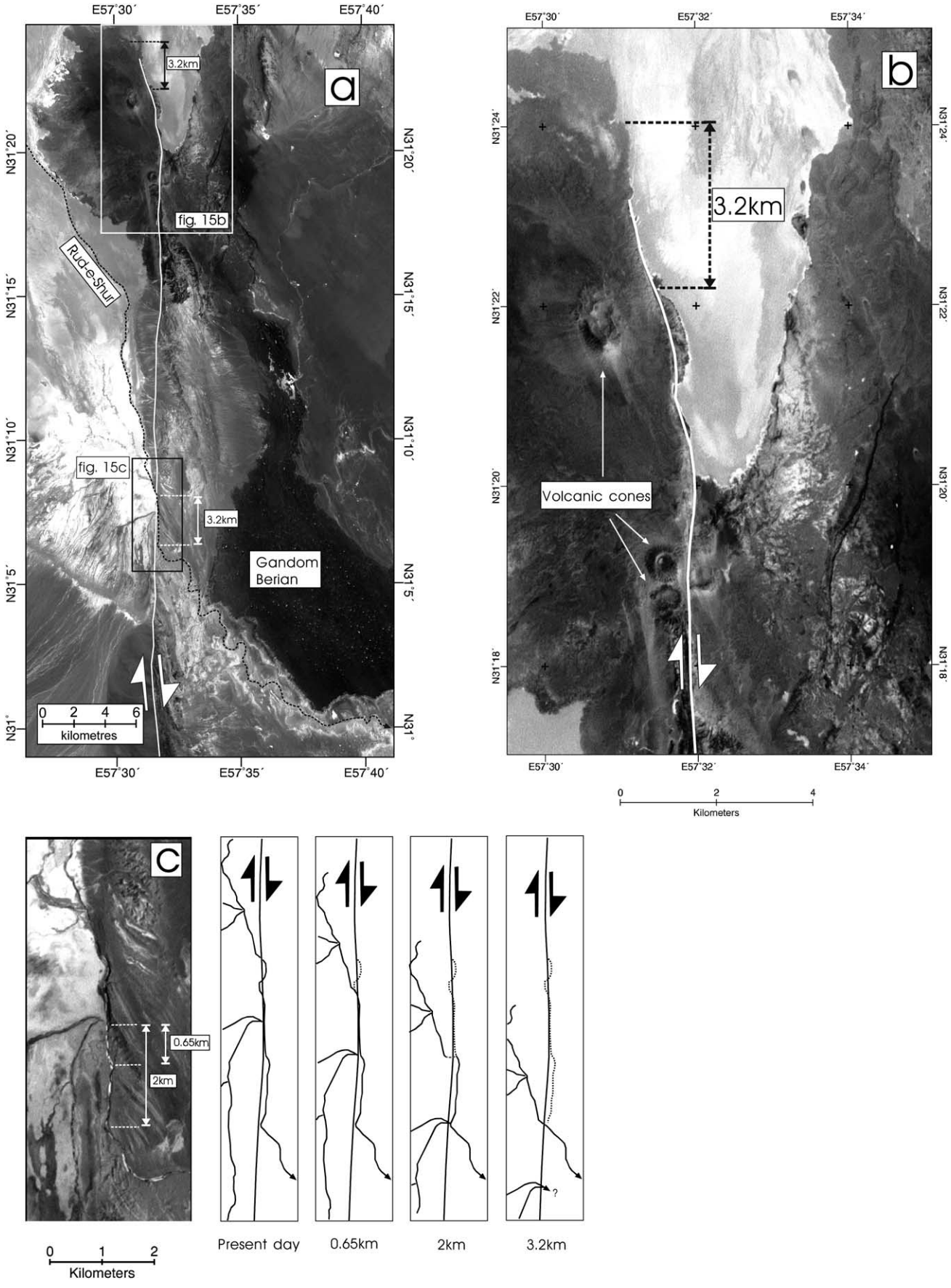
a
b
c
3.2km
fig. 15b
fig. 15c
Rudeh-Shur
Gandom Berian
Volcanic cones
0.65km
2km
0 2 4 6
kilometres
0 2 4
Kilometers
0 1 2
Kilometers
Present day
0.65km
2km
3.2km
E57°30´
E57°35´
E57°40´
E57°32´
E57°34´
N31°20´
N31°15´
N31°10´
N31°5´
N31°
N31°24´
N31°22´
N31°18´

on the Gowk fault is 12 km, giving a slip rate of ~2 mm/year if we assume the present-day tectonic configuration was initiated ~5 Ma ago. This estimate of cumulative offset is determined purely by restoration of geomorphic and drainage features (both active and abandoned), and yet is consistent both with offset bed-rock features at the southern end of the fault and with a slip-rate on the Nayband fault determined by K–Ar dating of basaltic rocks. The result is important for an understanding of Iranian tectonics, but also shows how fault evolution can be studied in detail using drainage systems. It is because the Gowk fault formed within the Abbarik–Sekonj mountains, so that the Abbarik range provided a barrier to the regional drainage, that the stream systems and geomorphology are so informative, enhancing the insights from analysis of seismology, radar and surface rupture data in earthquakes to give a more complete picture of the overall structure and kinematics of the faulting and how it evolves with time.

Acknowledgements

We would like to thank M.T. Khorehei and M. Qorashi of the Geological Survey of Iran in Tehran for their continued support and logistical help. M. Hoseini and the staff of GSI Kerman office were also most helpful and provided us with transport and accommodation. We are grateful to M. Talebian for his invaluable assistance both in Iran and Cambridge, to E. Fielding and B. Parsons for providing a digital elevation model for the region and to M. Berberian, K. Berryman, P. Knuepfer and R. Norris for helpful reviews. RW was supported by a NERC studentship. This work was supported by the NERC Centre for the Observation and Modelling of Earthquakes and Tectonics (COMET). This is Cambridge Earth Science Contribution No. ES 6527.

References

Aghanabati, A., 1993. Geological survey of Iran Geological quadrangle map of Iran No. J11 (Bam sheet), scale 1:250,000.

Ambraseys, N.N., Melville, C.P., 1982. A history of Persian earthquakes. Cambridge University Press.

Bayasgalan, A., Jackson, J., Ritz, J.-F., Carretier, S., 1999a. Field examples of strike-slip fault terminations in Mongolia and their tectonic significance. Tectonics 18, 394–411.

Bayasgalan, A., Jackson, J., Ritz, J.-F., Carretier, S., 1999b. 'Forebergs', flower structures, and the development of large intracontinental strike-slip faults: the Gurvan Bogd fault system in Mongolia. Journal of Structural Geology 21, 1285–1302.

Berberian, M., King, G.C.P., 1981. Towards a palaeogeography and tectonic evolution of Iran. Canadian Journal of Earth Sciences 18, 210–265.

Berberian, M., Qorashi, M., 1994. Coseismic fault-related folding during the South Golbaf earthquake of November 20, 1989, in southeast Iran. Geology 22, 531–534.

Berberian, M., Yeats, R.S., 1999. Patterns of historical earthquake rupture in the Iranian Plateau. Bulletin of the Seismological Society of America 89, 120–139.

Berberian, M., Jackson, J.A., Ghorashi, M., Kadjar, M.H., 1984. Field and telelseismic observations of the 1981 Golbaf–Sirch earthquakes in SE Iran. Geophysical Journal of the Royal Astronomical Society 77, 809–838.

Berberian, M., Baker, C., Fielding, E., Jackson, J.A., Parsons, B.E., Priestley, K., Qorashi, M., Talebian, M., Walker, R., Wright, T.J., 2001. The March 14 1998 Fandoqa earthquake (Mw6.6) in Kerman province, SE Iran: re-rupture of the 1981 Sirch earthquake fault, triggering of slip on adjacent thrusts, and the active tectonics of the Gowk fault zone. Geophysical Journal International 146, 371–398.

Burbank, D., Meigs, A., Brozovic, N., 1996. Interactions of growing folds and coeval depositional systems. Basin Research 8, 199–223.

Chu, D., Gordon, R.G., 1998. Current plate motions across the Red Sea. Geophysical Journal International 135, 313–328.

Conrad, G., Montigny, R., Thuizat, R., Westphal, M., 1981. Tertiary and Quaternary geodynamics of southern Lut (Iran) as deduced from palaeomagnetic, isotopic and structural data. Tectonics 75, T11–T17.

DeMets, C., Gordon, R.G., Argus, D.F., Stein, S., 1994. Effect of recent revisions to the geomagnetic reversal time scale on estimates of current plate motions. Geophysical Research Letters 21, 2191–2194.

Devlin, W.J., Cogswell, J.M., Gaskins, G.M., Isaksen, G.H., Pitcher, D.M., Puls, D.P., Stanley, K.O., Wall, G.R.T., 1999. South Caspian basin: young, cool, and full of promise. GSA Today 9, 1–9.

Dewey, J.F., Hempton, M.R., Kidd, W.S.F., Saroglu, F., Sengor, A.M.C., 1986. Shortening of continental lithosphere; the neotectonics of eastern Anatolia, a young collision zone. Special Publication of the Geological Society London 19, 3–36.

Dimitrijevic, M.D., 1973. Geology of Kerman Region. Institute for Geological and Mining Exploration and Investigation of Nuclear and Other Mineral Raw Materials. Report no. Yu/52, 1973, Belgrade.

Engdahl, E.R., van der Hilst, R., Buland, R., 1998. Global teleseismic earthquake relocation with improved travel times and procedures for depth determination. Bulletin of the Seismological Society of America 88, 722–743.

Falcon, N.L., 1969. Problems of the relationship between surface structure and deep displacements illustrated by the Zagros range. Special Publication of the Geological Society London 3, 9–22.

Falcon, N.L., 1974. Southern Iran: Zagros mountains. Special Publication of the Geological Society London 4, 199–211.

Freund, R., 1970. Rotation of strike slip faults in Sistan, southeast Iran. Journal of Geology 78, 188–200.

Griffis, R.J., 1981. Geological survey of Iran Geological quadrangle map of Iran No. J9 (Lakar Kuh sheet), scale 1:250,000.

Jackson, J.A., 1992. Partitioning of strike-slip and convergent motion between Eurasia and Arabia in Eastern Turkey and the Caucasus. Journal of Geophysical Research 97, 12,471–12,479.

Jackson, J., McKenzie, D., 1984. Active tectonics of the Alpine–Himalayan Belt between western Turkey and Pakistan. Geophysical Journal of the Royal Astronomical Society 77, 185–264.

Jackson, J., McKenzie, D., 1988. The relationship between plate motions and seismic moment tensors, and the rates of active deformation in the Mediterranean and Middle East. Geophysical Journal 93, 45–73.

Jackson, J., Haines, J., Holt, W., 1995. The accommodation of Arabia–Eurasia plate convergence in Iran. Journal of Geophysical Research 100, 15,205–15,219.

Fig. 15. (a) LANDSAT 7 image of part of the Nayband fault (see Fig. 3 for location). Quaternary basalts have flowed southeastward from volcanic cones along the fault zone to form the Gandom Berian plateau. Note that the Rud-e-Shur river course is deflected around the southern margin of the basalt. (b) Close-up view of the northern basalt margin. There is a maximum of 3.2 km offset of the basalt across the fault. (c) Close-up of the Rud-e-Shur river where it crosses the fault. A clear deflection of 3.2 km is seen. Intermediate drainage reconstructions for 2 km and 0.65 km of dextral displacement are also shown.

Jackson, J., Norris, R., Youngson, J., 1996. The structural evolution of active fault and fold systems in central Otago, New Zealand: evidence revealed by drainage patterns. Journal of Structural Geology 18, 217–234.

Jackson, J., Priestley, K., Allen, M., Berberian, M., 2002. Active tectonics of the South Caspian basin. Geophysical Journal International in press.

Jestin, F., Huchon, P., Gaulier, J.M., 1994. The Somalia plate and the East African Rift System: present-day kinematics. Geophysical Journal International 116, 637–654.

McCall, G.J.H., 1996. The inner Mesozoic to Eocene ocean of south and central Iran and associated microcontinents. Geotectonics 29, 490–499.

Mueller, K., Talling, P., 1997. Geomorphic evidence for tear faults accommodating lateral propagation of an active fault-bend fold, Wheeler Ridge, California. Journal of Structural Geology 19, 397–411.

Sahandi, M.R., 1992. Geological survey of Iran Geological quadrangle map of Iran No. J10 (Kerman sheet), scale 1:250,000.

Scholz, C.H., 1982. Scaling laws for large earthquakes: consequences for physical models. Bulletin of the Seismological Society of America 72, 1–14.

Tirrul, R., Bell, I.R., Griffis, R.J., Camp, V.E., 1983. The Sistan suture zone of eastern Iran. Geological Society of America Bulletin 94, 134–150.

Wellman, H.W., 1966. Active wrench faults of Iran, Afghanistan and Pakistan. Geologische Rundschau 18, 217–234.